UPPSALA
UNIVERSITET

UPTEC K 20025
Examensarbete 30 hp
Augusti 2020

Fused deposition modeling of API-loaded mesoporous magnesium carbonate

Andreas Abdelki

UPPSALA
UNIVERSITET

Teknisk- naturvetenskaplig fakultet
UTH-enheten

Besöksadress:
Ångströmlaboratoriet
Lägerhyddsvägen 1
Hus 4, Plan 0

Postadress:
Box 536
751 21 Uppsala

Telefon:
018 – 471 30 03

Telefax:
018 – 471 30 00

Hemsida:
http://www.teknat.uu.se/student

Abstract

Fused deposition modeling of API-loaded mesoporous magnesium carbonate

Andreas Abdelki

In this thesis, the incorporation of drug loaded mesoporous magnesium carbonate as an excipient for the additive manufacturing of oral tablets by fused deposition modeling was investigated. Cinnarizine, a BCS class II drug, was loaded into the pores of the mesoporous material via a soaking method, corresponding to a drug loading of 8.68 wt%. DSC measurements on the loaded material suggested that the drug was partially crystallized after incorporation, meanwhile the XRD diffractogram implied that the drug was in a state lacking long range order. The drug loaded material was combined with two pharmaceutical polymers, Aquasolve LG and Klucel ELF, and extruded into filaments with a single screw extruder. Filaments of Klucel ELF and drug loaded Upsalite (30:70 wt% ratio) were successfully implemented for the printing of oral tablets, in contrast to the Aquasolve LG based filaments which were difficult to print due to thickness variations and non-uniform material distributions. The drug content obtained by TGA suggested drug loadings of 7.71 wt% and 2.23 wt% in the drug loaded Upsalite and tablets respectively. Dissolution studies conducted with an USP II apparatus showed a slower API-release from the tablets in comparison to the crystalline drug, most probably due to slow diffusion of drug species through the polymeric matrix. For future studies, pharmaceutical polymers with higher aqueous solubility should be investigated in order to thoroughly examine the potential of utilizing the immediate release property of Upsalite.

Handledare: Ken Welch
Ämnesgranskare: Jonas Lindh
Examinator: Peter Broqvist
ISSN: 1650-8297, UPTEC K 20025
Tryckt av: Uppsala

Populärvetenskaplig sammanfattning

Läkemedel utgör en vital grund för den mänskliga hälsan, vilket skapar nödvändigheten till att effektivisera dess verkan i den mänskliga kroppen. Ett begrepp som kan användas för att beskriva hur effektivt ett läkemedel verkar vid intag är biotillgänglighet, vilket är den fraktion av läkemedel som når ut i blodet och genererar en terapeutisk effekt. Biotillgängligheten av oralt administrerade produkter kan förenklat beskrivas av två processer, vilka inkluderar substansens förmåga till att lösas upp i magtarmkanalen och diffusionen av substansen genom magtarmkanalens membranväggar för att slutligen nå ut i blodet. Ett betydande problem inom det farmaceutiska fältet är att en stor andel av redan befintliga läkemedel, likväl de i utvecklingsfasen, lider av låg vattenlöslighet som begränsar biotillgängligheten. Mycket av den forskning som bedrivs inom fältet idag kretsar därför kring att finna lösningar med syfte att öka vattenlösligheten hos läkemedelssubstanser.

En av dessa är att omvandla det fysikaliska tillståndet som substansen befinner sig i, vilket är från ett energetiskt stabilt kristallint tillstånd till ett metastabilt amorft tillstånd. Den termodynamiska drivkraften till bildandet av en lösning styrs av den energiminimering som processen i fråga genererar, vilket i fallet för ett amorft material blir högre bland annat på grund av dess metastabilitet. Det gör att amorfa läkemedel har en högre frisättningshastighet än dess kristallina motpart och kan därför resultera i en högre biotillgänglighet. Utmaningen med formulering av läkemedel i amorfa tillstånd är att de med tiden tenderar att återgå till det energetiskt fördelaktiga tillståndet, det kristallina tillståndet, likväl till följd av den termodynamiska drivkraften mot en energiminimering. En av de lösningar som givits stor uppmärksamhet är att stabilisera amorfa läkemedel i porösa material, där de inkorporeras i materialets porer och hindras från att kristallisera.

3D-printning är en additiv tillverkningsmetod vars princip går ut på att skapa ett tredimensionellt objekt genom en lager på lager metodik. Inom farmaceutiska tillämpningar förväntas tekniken konkurrera ut konventionellt massproducerande tillverkningsmetoder av orala formuleringar, genom att förändra tillvägagångssättet för hur design och tillverkning skall ske i framtiden. Tekniken öppnar upp dörren för nya strategier som potentiellt kan medföra en enhetsbaserad in-situ tillverkning av orala formuleringar som är skräddarsydda för patienten. Till skillnad från konventionella tekniker erbjuder additiv tillverkning fördelar som exempelvis en hög frihetsgrad i geometri och dimensionering av objektet, stor kontroll över distributionen av ingredienser i formuleringen, stor flexibilitet i antalet processbara materialklasser och en hög precision. Fused deposition modeling 3D-printing är en av många tekniker som finns tillgängliga, vars princip baseras på extrudering av termoplastiska filament som deponeras på en byggplatta lager för lager.

Syftet med detta projekt var att undersöka möjligheten till att producera filament bestående av det mesoporösa nanomaterialet Upsalite i kombination med en relevant farmaceutisk polymer för tillverkning av tabletter genom fused deposition modeling. Det lågt vattenlösliga läkemedlet cinnarizine inkorporerades i det porösa nätverket av Upsalite, varvid DSC-mätningar visade att en partiell kristallisering av läkemedlet hade skett. Det läkemedelsinkorporerade materialet kombinerades därefter med den farmaceutiska polymeren Klucel ELF, i ett förhållande på 30:70 viktsprocent, för att producera filament anpassade för implementering i 3D-printern. Cylindriska tabletter med 100% och 50% materialdensitet printades med filamentet. TG-analyser gav läkemedelskoncentrationer på 7.71 och 2.23 viktsprocent för Upsalite respektive den print-

ade tabletten. Frisättningstester av läkemedlet ur tabletterna visades erhålla lägre hastigheter i relation till det motsvarande kristallina läkemedlet och det inkorporerade läkemedlet, vilket högst troligt kan förklaras av polymerens inhiberande effekter.

Acknowledgements

I would like to begin by sending my appreciations to my supervisor Ken Welch, whose scientific approach was a joy to engage with, giving many stimulating and informative discussions over the course of this project. Furthermore, I would like to thank and credit him for the beautiful images captured with the SEM as well. I want to show my greatest gratitude towards Christos Katsiotis for supporting me immensely throughout the whole thesis, both his practical and theoretical knowledge within the field was of irreplaceable value for the successful outcome of this project. I would also like to extend my thanks towards my subject reader Jonas Lindh for his feedback on the report and my colleague Evgenii Tikhomirov for conducting the XRD-measurements.

Most importantly, I would like to thank my family and friends for always giving me their unconditional love and support, I truly share this accomplishment with you.

Contents

1 Introduction **1**
1.1 Aim . . . 1

2 Background **2**
2.1 Dissolution and solubility . . . 2
2.2 Bioavailability of oral formulations . . . 2
2.3 The biopharmaceutics classifications system . . . 3
2.4 Dissolution enhancement in the amorphous state . . . 3
2.5 Stabilizing amorphous drugs in mesoporous materials . . . 4
2.5.1 Mesoporous magnesium carbonate . . . 5
2.6 Fused deposition modelling 3D-printing . . . 6
2.6.1 Single screw extrusion . . . 7
2.7 Cinnarizine as active pharmaceutical ingredient . . . 7
2.8 Pharmaceutical grade polymers . . . 8
2.8.1 Hydroxypropyl cellulose . . . 8
2.8.2 Hydroxypropyl methylcellulose acetate succinate . . . 9

3 Experimental **10**
3.1 Materials . . . 10
3.2 API loading procedure . . . 10
3.3 Hot-melt extrusion . . . 10
3.4 FDM 3D printing . . . 10
3.5 Materials characterization . . . 11
3.5.1 Nitrogen gas sorption . . . 11
3.5.2 X-ray diffraction . . . 11
3.5.3 Scanning electron microscopy . . . 11
3.5.4 Fourier transform infrared spectroscopy . . . 11
3.5.5 Differential scanning calorimetry . . . 11
3.5.6 Thermal gravimetric analysis . . . 12
3.6 Calibration curve and solubility test . . . 12
3.7 Drug-release studies . . . 12

4 Results and discussion **13**
4.1 Structural characterization of API-loaded Upsalite . . . 13
4.2 Evaluation of the extrusion– and printing processes . . . 14
4.3 Characterization of extrudates and tablets . . . 17
4.4 Drug release from printed tablets . . . 19

5 Conclusion **22**

6 Future perspective **23**

Bibliography **27**

Appendix **28**

1 Introduction

Oral drug administration is the preferable route for medical treatment mainly due to patient compliancy, simplicity of intake and low cost. However, there are problems relating to the therapeutic efficiency of such dosage forms due to low bioavailability, which is defined as the fraction of unchanged administered active pharmaceutical ingredient (API) in the systematic circulation [1]. Bioavailability is determined by factors such as the aqueous solubility of the API, its dissolution rate and permeation through the membrane of the gastrointestinal tract. It has been estimated that up to 90% of drugs in the drug discovery pipelines are classed as poorly soluble in aqueous solutions [2]. This creates a rather significant issue with regard to the therapeutic efficiencies offered by orally administered drugs, since the active ingredient initially needs to dissolve in the gastrointestinal tract in order for the drug to be absorbed into the systematic circulation. Over the last decade, researchers have been trying to find new ways to effectively increase the solubility with the intention of enhancing the bioavailability of oral formulations. One of many strategies includes stabilization of drugs in their amorphous state, which has shown to increase the apparent solubility of drugs due to metastability and lack of a crystalline lattice. In recent decades, the stabilization of amorphous drug by incorporation into the pores of mesoporous materials has been investigated, entailing higher dissolution rates and stability due to geometrical restraint.

Additive manufacturing (AM) is a manufacturing technology based on the layer-by-layer deposition of materials, resulting in the formation of a three-dimensional object. It has previously been used as a rapid prototyping tool in different industrial fields but has in recent years garnered attention within the biomedical field due to its potential for manufacturing of oral dosage forms. Compared to conventional manufacturing technologies, additive manufacturing offers high flexibility when it comes to geometrical complexity, dimensions, precision, processable materials and compositional control of excipients. These, among other advantages, creates an opportunity for changing the way of how pharmaceutical formulation strategies will be approached in the future, possibly paving the way towards in situ personalized medicine. Fused deposition modelling 3D-printing (FDM 3DP) is an extrusion-based method that shows potential for the manufacturing of unit dosage forms due to its availability, low cost and versatility. It offers control over the API-distribution, dosage concentrations, shape and size, which makes it a promising tool for manufacturing of personalized medicine [3].

1.1 Aim

In this thesis, conducted at the division of nanotechnology and functional materials at Uppsala university, the feasibility of producing oral tablets using FDM 3DP by combining suitable pharmaceutical polymers and drug-loaded mesoporous magnesium carbonate has been investigated. Furthermore, the release properties of the crystalline drug, the amorphous drug incorporated into the mesoporous carrier and the tablet was studied.

2 Background

2.1 Dissolution and solubility

Solutions can be defined as the homogeneous dispersion of solute molecules within a solvent. For a solution to be generated at a molecular level, the interaction between the solute and solvent must result in the transfer of solute molecules from the solid state to the bulk of solvent, which is the process defined as dissolution. This is a kinetic property describing the change of concentration over time in the solvent bulk. The extent to which an infinite amount of solute can be dissolved in a given volume of the solvent, when thermodynamic equilibrium is established, is defined as its solubility [4]. The Noyes–Whitney equation (Eq.1) can be used to describe the rate of dissolution from spherical solid particles in relation to the solubility [5].

$$\frac{dC}{dt} = \frac{AD(C_s - C)}{h} \tag{1}$$

Where the dissolution rate dC/dt is defined as the rate of mass transfer through solvent boundary layers, A being the surface area of the dissolving particle, D its diffusion coefficient, h the thickness of the liquid boundary layer, C_s is the solubility and C the bulk concentration at a given time.

2.2 Bioavailability of oral formulations

Bioavailability is defined as the fraction of administered drug that reaches the systematic circulation unchanged, thus triggering a therapeutic effect. Compared to intravenous administration, in which the drug dose enters the systematic circulation immediately in full effect, orally administered drugs are not associated with generating high bioavailability. From the oral site of administration, the drug must pass through multiple stages of potential loss before resulting in a systematic absorption. The administered formulation must pass through the gut and dissolve in the intestinal fluids in order for drug species to transfer towards the gastrointestinal membrane, through which they permeate, to eventually reach the liver via the portal vein. Finally, the drug can either be metabolized by the liver or transported into the systematic circulation. The losses of orally administered drugs arising from this process is known as the first–pass effect [1].

Systematic absorption of orally administered drugs can be broken down to being primarily governed by dissolution and permeability through the intestinal membrane, although many underlying factors play part in the absorption kinetics. The driving force for systematic absorption is based on the molecular diffusion of drug species due to the concentration gradient created as the solid drug begins dissolving. Provided that dissolution is the rate limiting step, rather than permeation, an increase in dissolution rate would further increase this driving force, thus generating a higher absorption and possibly increasing the bioavailability of the drug. The dissolution rate is proportional to the solubility of a compound, as indicated by the Noyes–Whitney equation, which is the main reason as to why poorly soluble drugs are associated with low therapeutic efficiencies. In worst cases, the administered drug might not even have time to fully dissolve [1].

2.3 The biopharmaceutics classifications system

The biopharmaceutics classification system (BSC) was developed as a scientific framework aiming at understanding properties that determine the rate limiting steps of systematic absorption. This introduced the classification of drugs based on their aqueous solubility and intestinal permeability. Drugs are divided into four different groups as shown in Figure 1 [6]. Class II drugs are those which exhibit poor aqueous solubility and high permeation through the intestinal membrane, meaning that systematic absorption is primarily governed by dissolution. Therefore, drugs categorized in this specific class are of certain interest within the field of dissolution enhancement.

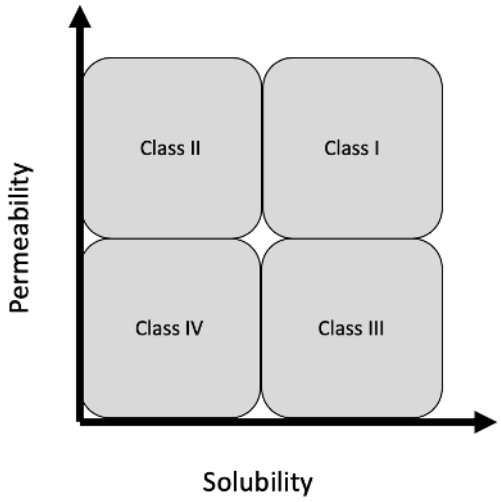

Figure 1: Graphic representation of the biopharmaceutical classification system

2.4 Dissolution enhancement in the amorphous state

The formation of a solution is thermodynamically driven and can be described by the change in free energy upon dissolution of crystalline material in a solvent. Equation 2 shows the relationship between the change in free energy (ΔG), change in enthalpy (ΔH) and entropy (ΔS).

$$\Delta G = \Delta H - T\Delta S \tag{2}$$

One of many complex processes that constitutes the dissolution of crystalline materials is the release of individual atoms from the crystalline lattice, which is an endothermic process. The fragmentation of the crystalline lattice is thus associated with an energy barrier that needs to be overcome, simply referred to as the lattice enthalpy [4, 7]. The positive enthalpic contribution generated by this specific process will therefore give a positive contribution to the change in Gibbs free energy. In contrast to solid crystals, amorphous materials are characterized by their lack of long-range order, i.e. being comprised of molecules or atoms that are not structurally arranged in accordance with a lattice pattern. An amorphous material exists in a higher state of free energy making it more unstable, which in combination with the lack of a crystal lattice results in an enhanced dissolution compared to its crystalline counterpart [8, 9]. The dissolution

rate increases to such high degrees that the concentration of the solution will exceed the thermodynamic solubility, given that enough material is used. This results in the increased apparent solubility of the drug, creating a supersaturated solution in a metastable state (Figure 2). As a result, the content of dissolved species will eventually decrease to the equilibrium concentration due to the driving force of recrystallization, resulting in precipitation of the drug. However, the supersaturated state can be maintained long enough for the systematic absorption to increase, thus improving the bioavailability of the administered drug [10, 11, 12]. The main challenge relating to amorphous formulations is their inherent instability upon storage, since the structure tend to transition from the metastable state to a more energetically favorable one over time.

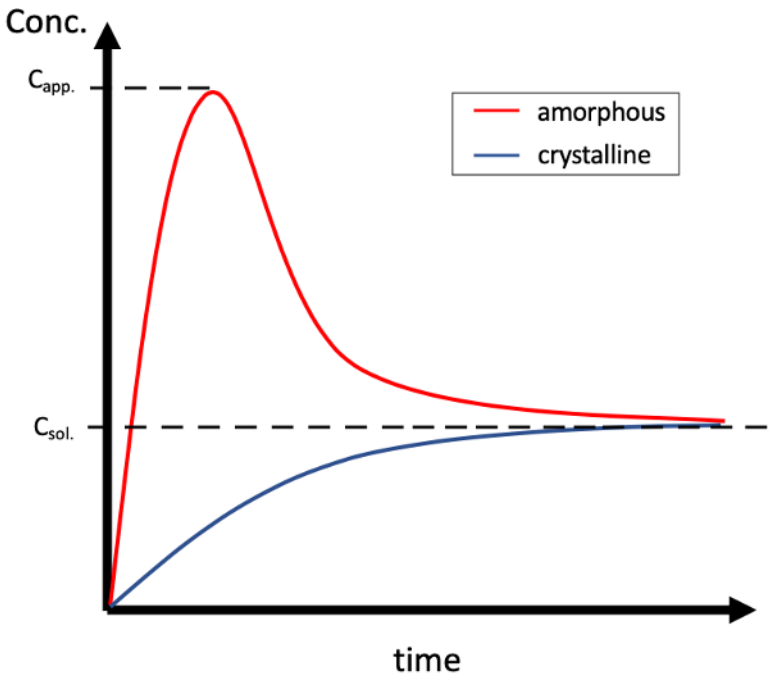

Figure 2: The dissolution profile of amorphous (red) versus crystalline (blue) drugs. The thermodynamic solubility is denoted $C_{sol.}$ and the increased apparent solubility $C_{app.}$.

2.5 Stabilizing amorphous drugs in mesoporous materials

Investigations regarding the drug loading of porous materials were made as early as 1984. In this specific paper, XRD and DSC were utilized in order to study the physical state of benzoic acid incorporated into the pore network of controlled pore glass (CPG). The measurements showed that the incorporated drug was present in an amorphous state within the porous material. [13]. It was later shown that the drug was more prone to exist in an amorphous state when incorporated into pore networks with sizes in the mesoporous range, i.e. 2-50 nm [14]. Further advances in the manufacturing of porous materials gave rise to the discovery of silica-based mesoporous materials, including the MCM–41 which was later proposed as potential drug delivery vehicle due to the successful incorporation and release experiments of ibuprofen [15]. Since then, different types of mesoporous silicas have been successfully utilized to incorporate drugs in the amorphous state, suppressing crystallization and increasing their apparent solubility [16, 17, 18]. The synthesis of mesoporous silica materials relies on the utilization of assembled amphiphilic organic molecules (surfactants) as pore-forming–and structure-directing agents, giving good control over pore-size distributions and structural morphology. However,

the production is associated with high costs and environmental issues, due to expensive silica precursors and the pore-forming templates that are often both expensive and toxic [19].

Mesoporous materials possess high specific surface areas (SSA), thus high surface energies, and the absorption of an amorphous drug is believed to generate a larger reduction in the total free energy in comparison to its crystalline counterpart [20, 21]. Upon loading of the drug, molecules are deposited onto the channel walls through different kinds of interactions, which will initially result in the formation of a drug monolayer [22]. Once all of the active sites on the pore walls are occupied, excess drug molecules will continuously form amorphous drug layers onto the prior ones until the pores are filled. These excessive amorphous layers are suggested to be stabilized due to geometrical restraint, thus inhibiting the naturally expected crystallization [23]. With respect to the pore filling mechanism, the drug loading capacity of a mesoporous material is dictated by two separate material properties [24, 25]. The number of active sites on the pore walls are proportional to the SSA of the material, which suggest that the monolayer drug loading capacity is determined by the specific surface area. In contrast, the amount of excess-drug filling up the pores, referred to as the pore filling capacity, is determined by the pore size. Further addition of drug will cause an overload and result in the crystallization of drug molecules residing on the outer surface.

2.5.1 Mesoporous magnesium carbonate

Mesoporous magnesium carbonate, marketed as Upsalite, is an amorphous nanostructured material with a narrow pore size distribution of 6–8 nm and a SSA typically between 300–800 m^2/g [26]. It is synthesized by a template-free, low temperature process using methanol, carbon dioxide and magnesium oxide as precursors. In short, the magnesium carbonate is formed by a sequence of reactions involving methanol and magnesium oxide in a carbon dioxide pressurized environment below 100°C [27]. This sequence creates an intermediate product $Mg(OCOOCH_3)(OCH_3)$) that physically binds carbon dioxide, which evaporates together with methanol during a solidification step, resulting in the formation of a randomly arranged pore network in the mesoporous range [28].

In 2014, ibuprofen was successfully loaded and confined in an amorphous state within the pore network of Upsalite [29]. The mesoporous material displayed a stabilizing effect on the drug, indicated by the lack of crystallization after storing the formulation in 75% relative humidity over a three-month period. Dissolution studies of Ibuprofen showed a rapid initial release of the drug, as indicated by its amorphous nature, that exceeded the rate of its crystalline counterpart. Later, the potential of using Upsalite as a drug delivery vehicle for other poorly soluble class II drugs was investigated. In vivo dissolution studies of cinnarizine, celecoxib and griseofulvin resulted in supersaturated solutions as expected, displaying a concentration–maxima corresponding to an apparent solubility that was almost 3 times higher than the measured thermodynamic solubility [30]. When estimating the amount of drug released from time zero up to the point of which the supersaturated solution eventually reached equilibrium, the drug content due to dissolution from Upsalite was significantly higher than the amounts generated from the corresponding crystalline drug. In order to prolong the supersaturated state, in vitro dissolution studies were conducted to investigate the effect of incorporating hydroxypropyl methylcellulose (HPMC) as a crystal inhibitor [31]. The suppressed crystallization when utilizing the polymer was evident, since the release profile was indicative of the so-called parachute effect, in which the non-equilibrium concentrations are maintained for a longer period of time.

2.6 Fused deposition modelling 3D-printing

Fused deposition modelling 3D–printing (FDM 3DP) is one of many additive manufacturing technologies based on the characteristic layer-by-layer production of components. More specifically, the process is done by extrusion of thermoplastic filaments through a nozzle. The filament is mechanically fed in towards a heating element (heat block) where the polymer softens/melts and is vertically extruded from the printer nozzle, resulting in a two-dimensional layer deposition onto the builder plate. The vertical deposition of molten material continuously proceeds in the same manner, resulting in a time efficient and high precision layer-by-layer production of a three-dimensional structure possessing good mechanical properties [32]. Figure 3 shows a simplified set-up of the FDM-printer. Hot–melt extrusion (HME) technology is commonly coupled with FDM 3DP to produce suitable filaments.

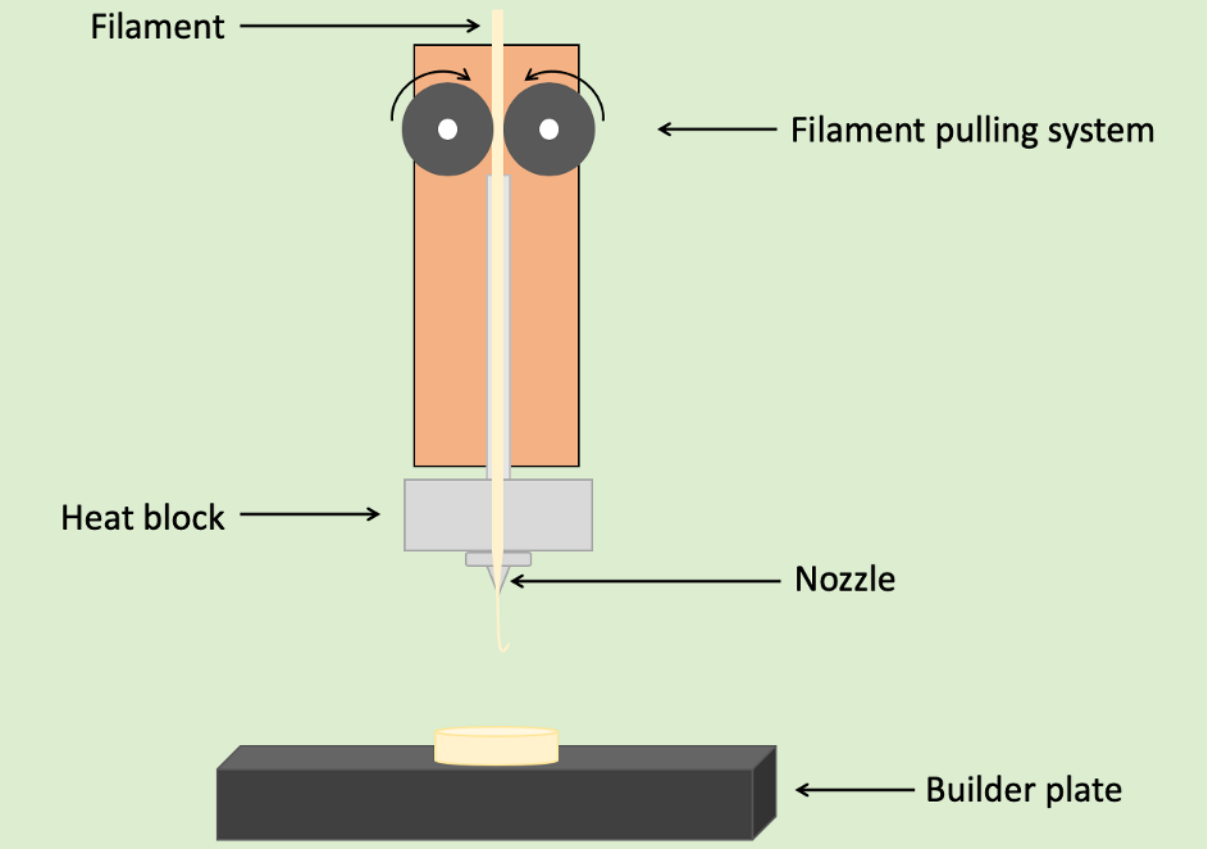

Figure 3: General layout of the FDM-printer.

In recent years, FDM 3DP has garnered an increase in interest within the pharmaceutical research field, due to its manufacturing potential of single unit dosage forms [33]. It presents the possibility of manipulating a variety of parameters such as geometry, dimensions and density of the final product, including parameters relating to the dose and distribution of API. The fact that it possesses such high versatility with respect to formulation of dosage forms, makes the technique promising for development of personalized medicine [3]. Most of the early research within the field centered around the feasibility of using solid dispersions of drugs contained within polymeric matrices, as a means to print oral dosage forms. Initially, drug loading procedures were conducted by incubation of HME-produced PVA-filaments in drug dissolved organic solvents, in which the loading mechanism occurs through passive diffusion of drug molecules

into the filament [34, 35, 36]. However, this method showed to be both time consuming and underwhelming with regards to the generated yields of loaded drug concentrations. The outcome of these studies paved the way for an alternative approach for producing amorphous solid dispersion-based filaments, which was the successful utilization of HME to extrude mixtures and thus loading the drug by means of thermal treatment [37]. Although generating higher drug concentrations, the preparation of such filaments increases the probability of drug degradation due to thermal processing [38]. Further advances were extended towards screening of different pharmaceutical grade polymers such as cellulose derivatives (EC, HPC, HPMC, HPMCAS), methacrylic based polymers (Eudragit) and polyethylene glycols (PEG) [3, 39, 40]. However, the majority of pharmaceutically relevant polymers available today do not exhibit desirable mechanical properties, which creates the necessity of incorporating other excipients. This is probably the most significant disadvantage relating to the manufacturing of oral drug formulations with FDM 3DP, since an optimized printing process is mostly dependent on finding a processable composition [38].

2.6.1 Single screw extrusion

The working principle of an extruder is based on the shaping of molten polymeric material into a solid object in accordance with the specified dimensions of a die. Solid material is fed in through a hopper and subjected to elevated temperatures once in the barrel, due external heating components and mechanical friction. The movement of molten material along the barrel direction is induced by the rotating screw, thus being transferred towards the die where it eventually is pushed through, resulting in the formation of a solid object with specified dimensions once cooled down [41]. Figure 4 shows the basic setup of a single screw extruder.

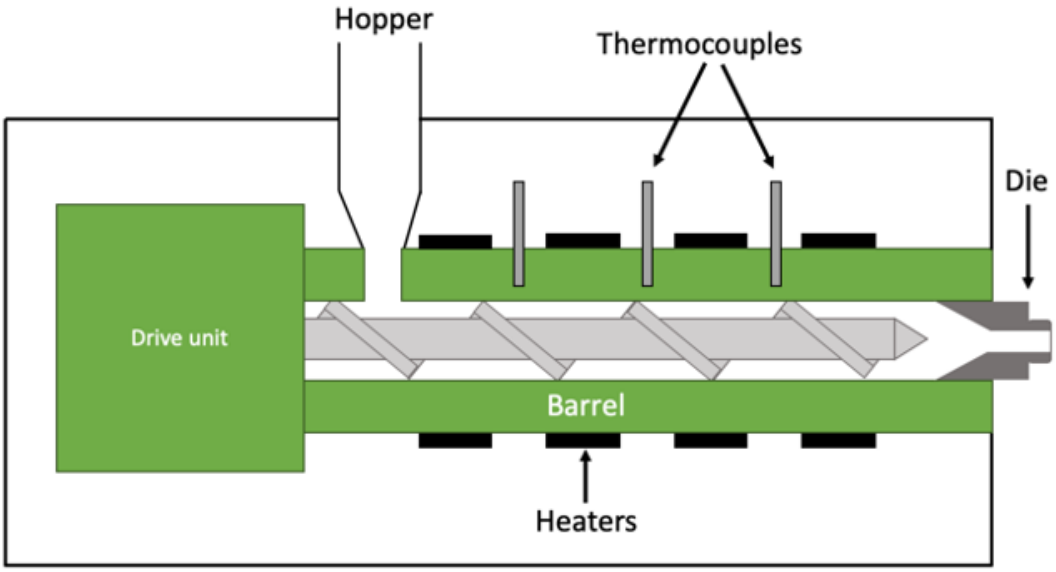

Figure 4: Single screw extruder

2.7 Cinnarizine as active pharmaceutical ingredient

Cinnarizine is a drug with antihistaminic properties and calcium channel blocking ability and is primarily used for treating nausea and vomiting [42]. It is a lipophilic weak base and exhibits low solubility at pH-values over 5.5, thus being classified as a class II drug in the BCS [43].

Figure 5 shows the chemical structure of cinnarizine and Table 1 lists its relevant physicochemical properties.

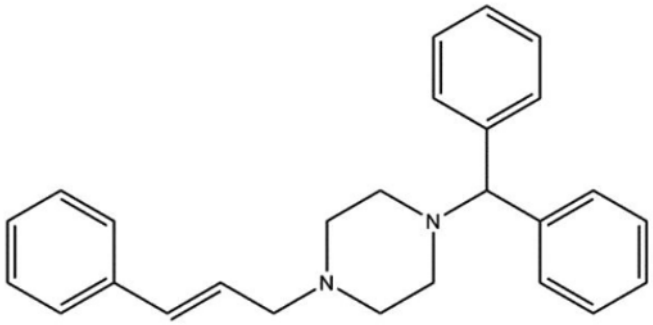

Figure 5: Chemical strucure of Cinnarizine.

Table 1: Physicochemical properties of cinnarizine.

Aqueous solubility [mg/L]	pKa	M_w [g/mol]	T_m [°C]
<1[a]	7.45[b]	368.5[b]	120[b]

[a] obtained from reference [44]
[b] obtained from reference [45]

2.8 Pharmaceutical grade polymers

2.8.1 Hydroxypropyl cellulose

Hydroxypropyl cellulose (HPC) is a non-ionic water soluble cellulose ether containing hydroxypropylated functional groups on the cellulose backbone (Figure 6). Compared to other water-soluble polymers, HPC is more hydrophobic due to the hydroxypropyl substituents. It follows the dissolution mechanism of swelling and erosion. Different grades of HPC are commercially offered by Ashland, marketed as Klucel HPC, with the main difference being the molecular weights ranging from 40–1150 kDa. Lower molecular weight compounds have a lower melt viscosity, which simplifies the processability at lower temperatures. Klucel HPC exhibits a dual glass transition temperature, where the true Tg is around 150°C, while a beta transition occurs close to 0°C due to side chain activity, which might explain its increased plasticity and flexibility [46].

HPC is widely used in the conventional manufacturing of oral formulations as a film former, tablet binder, film coating and extended release–matrix former [46]. In FDM 3DP related studies, the feasibility of using HPC (Klucel LF) was explored by using HME-produced filaments to successfully produce printed oral capsular devices [47]. Later, Theophylline loaded HPC SSL (40 kDa) were printed in a capsular shape and in vitro dissolved, showing promising results for the application as an immediate release drug delivery system, as closer to 90% of the loaded drug was dissolved in 100 minutes [39]. Since then, different grades of HPC have been combined with other pharmaceutical polymers for producing extended-release tablets, immediate-release hollow structures and sustained-release tablets [48, 49, 50].

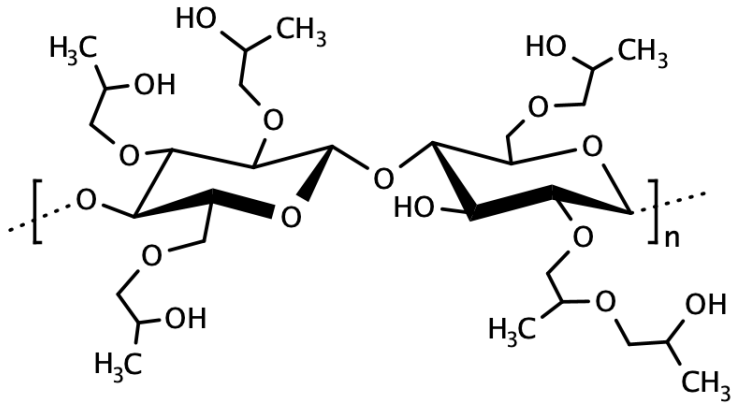

Figure 6: Chemical structure of the monomeric unit of HPC

2.8.2 Hydroxypropyl methylcellulose acetate succinate

Hydroxypropyl methylcellulose acetate succinate (HPMCAS) is a synthetic polymer derived from cellulose (Figure 7). More specifically, it is a mixture of acetic acid and monosuccinic acid esters of hydroxypropyl methylcellulose. HPMCAS is an enteric polymer, meaning that it is insoluble in gastric pH but dissolves in intestinal pH by swelling. The polymer is commercially marketed as Aquasolve HPMCAS and comes in different grades based on the ratio between acetyl and succinoyl functional groups. All grades show a glass transition temperature at around 120°C [51].

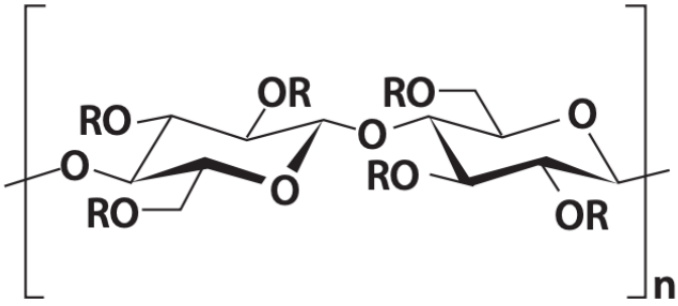

R= H, CH_3, $C(O)CH_3$, $C(O)CH_2CH_2CO_2H$ or $[CH_2CH(CH_3)O]_mR$

Figure 7: Chemical structure of the monomeric unit of HPMCAS.

HPMCAS is widely used as an enteric coater for tablets and capsules. In recent years, it has gained attraction due to its parachute property, i.e. the ability to maintain a supersaturated state over a longer period of time as described previously [52, 53]. In the quest of exploring new formulation strategies, the material has also been investigated within the field of FDM 3DP. Paracetamol loaded HPMCAS filaments of different grades were printed into tablets, showing a delayed release profile as expected due to its pH-responsiveness. The dissolution rate of the drug was also shown to increase for grades with higher succinoyl content once introduced to intestinal conditions [40].

3 Experimental

3.1 Materials

Klucel ELF, AquaSolve LG and Plasdone S-630 were kindly donated from Jonas Lindh. PVP K12, magnesium carbonate, disodium phosphate (DSP), monosodium phosphate (MSP), sodium dodecyl sulfate (SDS), hydrochloric acid (HCl) were all purchased from Sigma Aldrich. PEG 400 and magnesium stearate were purchased from Alfa Aesar. Mesoporous magnesium carbonate was provided through a donation by Disruptive materials AB.

3.2 API loading procedure

Prior to the loading process, Upsalite was thermally treated in an oven for 24 hours in 85°C for the removal of humid residues. Upsalite was loaded with cinnarizine through a soaking method, in which 2.9 grams of cinnarizine was dissolved under magnetic stirring in 1300 ml concentrated ethanol, thus corresponding to a concentration of 2.2 mg/L. Once dissolved, 30.5 grams of Upsalite was added to the mixture and left stirring for approximately 48 hours at 48°C. Subsequently, rotary evaporation was utilized to separate the loaded Upsalite particles from the ethanol solution, which was carried out at 40°C and 150 rpm. Lastly, the API–loaded Upsalite was dried over night at 90°C.

3.3 Hot-melt extrusion

Various compositions based on the Klucel ELF and AquaSolve LG were extruded, which are listed in table 4 in appendix. Other pharmaceutical grade polymers (PVP K12, Plasdone S-630) were also extruded but dismissed due to time constraints. The general approach of the extrusion processes was to conduct experiments with samples containing only the pharmaceutical polymers and using these results in order to find suitable additives for generating a filament with desirable properties. Once in the stage of incorporating the mesoporous material into the mixture, the experiments were initially conducted with magnesium carbonate and unloaded Upsalite, after which the API-loaded Upsalite was incorporated. All samples were manually mixed with a mortar and pestle in order to achieve a homogenous mixture as well as to grind agglomerated particles present in both materials. The mixtures were extruded into continuous filaments with the Filabot EX2 single screw extruder, using a die with 1.5 mm in diameter. Initial temperature settings were chosen based on previous literary work and the polymers respective glass transition temperatures. Thereafter, extrusion temperatures were optimized by trial and error to the point of obtaining a desirable material flow through the die. Similarly, the extrusion speeds were chosen through a process of optimization, primarily in order to obtain desirable filament thicknesses.

3.4 FDM 3D printing

Similar to the approach of finding optimal extrusion temperatures, initial printing and bed temperatures were chosen with the basis of increasing the flow of molten material in relation to the flow obtained with temperatures used during extrusion. The temperature settings where thereafter optimized in a trial and error manner to obtain both printing and bed temperatures that would result in good flow and layer binding. Flat cylindrical shaped tablets were designed using Autodesk Maya 2019. The template was exported as an object file (.obj) into the open-source slicing software PrusaSlicer (version 2.2.1+), in order to create a geometrical code (.gcode)

that contains all the information. The tablet diameter and thickness were selected to be 11 mm and 3 mm respectively. Oral formulations of 100%– and 50% infill densities were printed with appropriate filaments using the Original Prusa i3 MK3S FDM 3D printer.

3.5 Materials characterization

3.5.1 Nitrogen gas sorption

In this study, nitrogen gas sorption was used to characterize the porous properties of the unloaded and API–loaded Upsalite. Gas sorption isotherms were recorded using the ASAP 2020 V4.03 instrument at –196°C. Degassing of the samples were conducted at 85°C for 10 hours prior to analysis. Brunauer–Emmet–Teller (BET) method was employed in the relative pressure ranges between 0.05 and 0.3 when calculating the SSA, whereas the pore size distribution was recorded using density functional theory (DFT). The total pore volume was obtained using a single point absorption at relative pressures 1.

3.5.2 X-ray diffraction

Powder XRD was utilized in order to analyze the physical state of the drug prior and after loading into Upsalite. Pulverized material was thoroughly distributed on a sample holder made of glass in order to create an even and flat surface. The experiments were conducted with the Siemens/Bruker D5000 X-ray diffractometer (45 kV, 40 mA) in a 2θ range of 5–90°, with a step size of 0.05°measured in 0.5 seconds.

3.5.3 Scanning electron microscopy

In this work, SEM was performed with a Zeiss Leo 1550 SEM operating at an acceleration voltage of 5 keV. Samples were first sputter coated with a thin layer of gold/palladium to minimize charging effects.

3.5.4 Fourier transform infrared spectroscopy

Bruker tensor 27 spectrometer was utilized in order to characterize the chemical structures of raw materials, and in relation these results, study the possibility of chemical changes in the API loaded Upsalite, filament and tablet. Prior to the sample analysis, a background scan with an empty sample holder was conducted. An attenuated total reflectance (ATR) spectrum for wavelengths ranging from 400–4000 cm^{-1} was obtained, using 128 scans with a resolution of 4 cm^{-1}.

3.5.5 Differential scanning calorimetry

In this thesis, DSC was employed as a complement to the XRD–measurements, i.e. to further characterize the physical state of the incorporated drug. Sample preparations included manually weighing of the material in aluminum pans and subsequently enclosing them with a press prior to analysis. All experiments were conducted with a Mettler Toledo DSC 3 instrument in an inert nitrogen environment using a gas flow of 60 ml/min and temperatures ranging from -35–300°C at a rate of 10°C/min.

3.5.6 Thermal gravimetric analysis

TGA was used for both characterization of thermal properties and calculation of the loaded drug content. Ceramic crucibles where used as carriers and the experiments were conducted with the Mettler Toledo TGA 2–instrument. The method employed consisted of a dynamic temperature profile ranging between 35–600°C with a heat rate of 10°C/min, and a static profile at the final temperature for 30 minutes. All experiments were performed in an air-based environment with a flow rate of 40 ml/min.

3.6 Calibration curve and solubility test

The calibration curve was obtained through absorption measurements of drug solutions with given concentrations prepared from stock. The drug was dissolved in phosphate buffered saline (PBS) containing 0.05 wt% sodium dodecyl sulfate (SDS). The experiments where conducted with an UV-1800 Shimadzu spectrophotometer at 252 nm.

Solubility studies were conducted by dissolving an excess amount of crystalline cinnarizine in the PBS-based buffer, which was then left for stirring in 200 rpm and 37°C for 48 hours. Samples were collected from the bulk with a syringe and filtered with polyethersulfone membranes with pore sizes of 0.45 m prior to the UV/VIS measurement.

3.7 Drug-release studies

Standard release studies of crystalline cinnarizine, drug loaded Upsalite, 50% infill tablets and 100% infill tablets were conducted at 37°C and 50 rpm using a Sotax dissolution bath (USP II apparatus) equipped with 1000 ml vessels. The samples were dissolved in 900 ml of 0.1 M PBS containing 0.05 wt% SDS, which was added in order to increase surface wetting and improve absorption detection. With the intention of simulating the environment of the small intestine, the dissolution media was set to a pH-value of 6.8. Experiments were conducted in triplicates, with sample masses corresponding to the drug loading of 50– and 100% infill tablets, which are given in Table 2. Experiments with unloaded Upsalite and tablets were conducted in the same manner, corresponding to control samples. For each sampling, aliquots of 3 mL were extracted from the vessels using a syringe, wherein the vessels where replenished with 3 mL of pure buffer solution. Prior to absorption analysis with UV/VIS spectrophotometry, the extracted samples were filtered using polyethersulfone membranes with pore sizes of 0.45 m.

Table 2: Sample-weights that were used during release studies. The weight of the tablets correspond to the average weight of 5 different printed tablets with respective infill density. The weight of crystalline API and loaded Upsalite samples were calculated with respect to the tablet composition and drug content in Upsalite.

	Cinnarizine	Loaded Upsalite	Tablet
Weight (50% infill)	4.33 mg	49.9 mg	166±4 mg
Weight (100% infill)	7.05 mg	81.2 mg	270±4 mg

4 Results and discussion

4.1 Structural characterization of API-loaded Upsalite

Figure 8 shows the XRD patterns (a) and DSC curves (b) for the crystalline cinnarizine, unloaded Upsalite and API-loaded Upsalite. The diffractogram of the unloaded Upsalite exhibits crystalline peaks at 43– and 62°corresponding to trace amounts of MgO from synthesis [27]. The lack of other peaks and the presence of a halo at 30°confirms that the Upsalite contains an amorphous phase of magnesium carbonate. Upon API-loading, no trace of crystalline peaks corresponding to cinnarizine can be observed, which indicates that the drug is present in a state lacking long-range order and has thus been successfully incorporated into the Upsalite pore network [26, 29]. DSC–measurements conducted on crystalline cinnarizine gave an endothermic peak at 121°C, corresponding to the melting point of the substance [30, 45]. The same peak can be seen for the API-loaded Upsalite, which in contrast to the diffractogram suggests that the drug was not completely incorporated in an amorphous state. This indicates that the API was partially crystallized, most probably on the surface of the Upsalite particles.

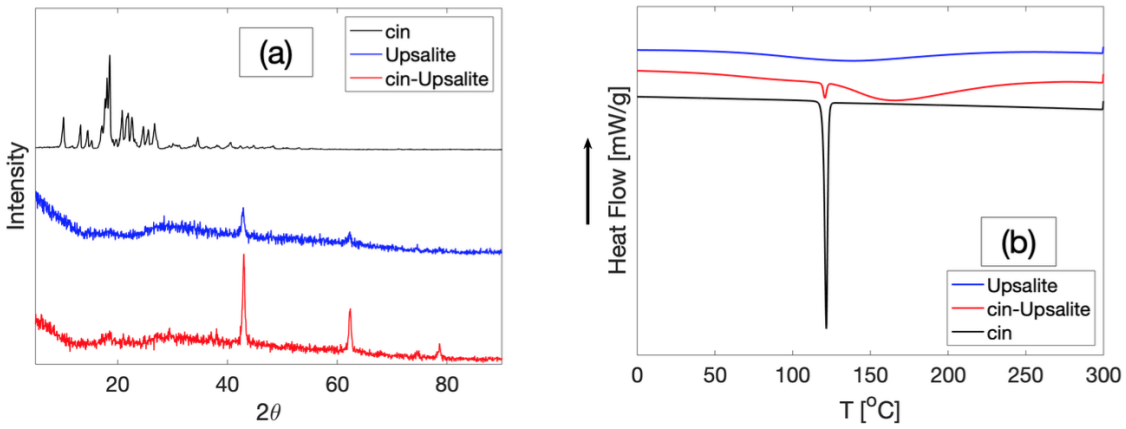

Figure 8: (a) XRD measurements on the API, unloaded Upsalite and the API-loaded Upsalite. The results indicate that the drug was incorporated into the pores of Upsalite in an amorphous state. (b) Corresponding DSC measurements show that the incorporated drug was partially crystallized during the process.

BET specific surface area and single point pore volume obtained by the N_2–sorption measurements are given in Table 3. Both parameters were reduced upon loading of the drug, as is expected by the adsorption of API onto the pore walls of the mesoporous carrier. A reduction in pore volume of approximately 52% was observed, i.e. half of the pore volume available prior to the loading procedure was filled by the drug. The amount of empty pore volume left suggests that a larger amount of cinnarizine could be incorporated. Furthermore, these results combined with the knowledge of how the pore filling mechanism works would contradict the presence of a crystalline state. In the field of pharmaceutical science, a classification system of crystalline tendencies over a wide variety of pharmaceutical compounds was developed as a framework for assessing the viability of an amorphous formulation. This was done by thermal treatment of supercooled cinnarizine (among other compounds) using a DSC-instrument with heat rates of 10 °C/min, which showed to crystallize the drug during the heating stage [54]. As a result, cinnarizine was characterized as a class (II) compound, meaning that it is prone to crystallize

upon heating at temperatures over its Tg. Thus, its crystallization tendency could act as a plausible explanation for the presence of the crystalline phase indicated by the DSC-curve of the drug-loaded Upsalite, particularly with respect to the obtained XRD results.

Table 3: The BET SSA and single point pore volume for the unloaded– and loaded Upsalite.

	Unloaded Upsalite	Loaded Upsalite
SSA $[m^2/g]$	213.9662±2.6715	73.0006±0.8101
Pore volume $[cm^3/g]$	0.304413	0.158180

4.2 Evaluation of the extrusion– and printing processes

In this section, the properties of extruded filaments are studied in relation to their printability. A variety of different polymers were investigated by extrusion to assess the potential of incorporating Upsalite, with the eventual aim of producing suitable filaments for the printing process. Plasdone S-630 and PVP K12 were dismissed from further compositional development due to time constraint, since undesirable brittleness would lead to a time-consuming process.

Extrusions of AquaSolve LG were conducted at temperature ranges between 120-165°C with varying extrusion rates, resulting in relatively brittle filaments. PEG 400 was used as a plasticizer to increase its ductility, accounting not only for the inherent brittleness of the polymer, but also for the expected increase in brittleness that the addition of Upsalite would entail. Extrusions of physical mixtures containing both unloaded– and loaded Upsalite resulted in filaments exhibiting non-uniform material distributions and thickness variations. One of the phenomena observed during the extrusion of these mixtures was the formation of a white coating along the perimeter of the filament. The color gradient ranging from white to brown along the filament cross section suggests that it was composed of a polymer core with an increasing amount of Upsalite particles closer to the perimeter. The surface of the filament would increase in coarseness with the length of the filament as shown in Figure 9 (a), which means that the outer surface of the filament indeed was comprised of Upsalite. Furthermore, a brittle coating was formed on the extruder walls, which is shown in Figure 10 (a). These phenomena verify an uneven material distribution along two directions in total, i.e. along the cross section of the filament and its length. The explanation for this could be that the low miscibility between the two materials inhibits the Upsalite particles to fully disperse into the polymer melt, resulting in the repulsion of particles towards the extruder walls. As a result, the movement of these particles was probably inhibited due to frictional forces arising from the interaction with the extruder walls. This would most likely generate an outer layer comprised of Upsalite, with an increasing concentration towards the end part of the filament. In order to combat the issue of uneven concentrations along the filament length, magnesium stearate was implemented into the mixture as a lubricant. Unfortunately, the addition of the compound did not yield the desired outcome.

The die–swelling effect was observed when extruding the AquaSolve, which is a phenomenon caused by the inability of entangled polymer chains to orient along the flow direction as the material is forced through a narrow die, originating from its viscoelastic nature [55]. This property is determined by the relaxation time, which is the characteristic time needed for the polymer to relax into a stress–free state during deformation. Polymers with larger molecular weights tend to have a longer relaxation time, thus resulting in a more prominent die swell. Figure 10 (b) shows the resulting die swell during extrusion of a mixture containing loaded Upsalite and AquaSolve

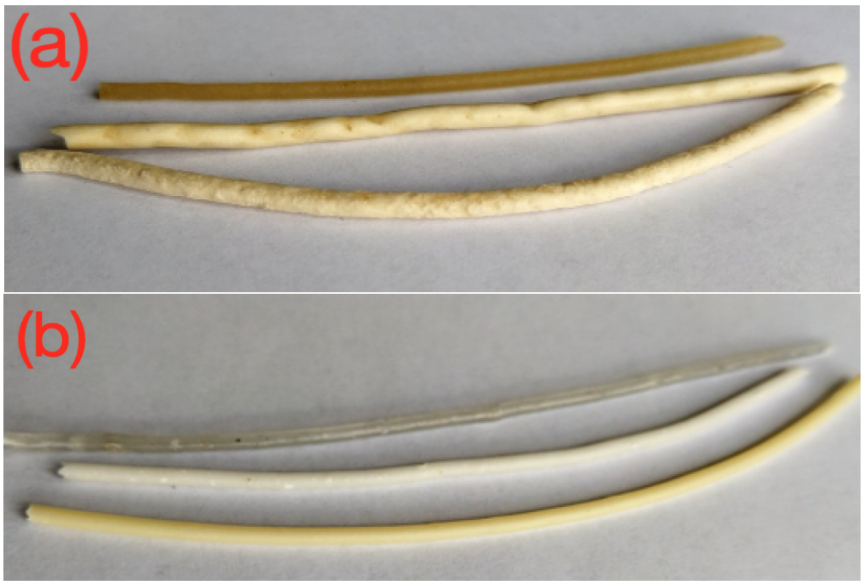

Figure 9: (a) Ordering filaments beginning from the top: 100 wt% AquaSolve LG; First part of the filament containing 30 wt% loaded Upsalite and 70 wt% Aquasolve LG; End part of the same filament. The first part of the loaded filament exhibiting local thickness variations and a relative smooth surface. In contrast, the end part of the filament being coarser. (b) Ordering from the top: Raw Klucel ELF; 30/70 wt% of unloaded Upsalite and Klucel respectively; The same composition with API-loaded Upsalite instead. The smooth surface of the API-loaded Klucel-filament is evident when comparing it to the corresponding AquaSolve-filament.

LG (30:70 wt%). The die diameter used was 1.5 mm, resulting in an average filament thickness of 2.30 mm, compared to the 1.55 mm filament thickness obtained with the corresponding composition based on Klucel ELF. The relaxation time is proportional to the extrusion speed, so in order to account for this effect the extrusion speed was reduced, causing a more time-consuming process. Printing trials at varying temperatures with the drug-loaded AquaSolve filament were eventually conducted. Initially, implementation of the filament showed to be promising as it was successfully loaded into the printer head, hence extruding molten material through the nozzle. However, the flow of molten material would stop in the early stages of the printing process. The printer head was disassembled in order to identify the cause of this problem, which was confirmed to arise from the clogging of molten material inside the heat break, which is the component that connects the cold–and hot-end parts of the printer. Further observations showed that the clogged material was mainly comprised of a brittle powder, which indicated that local agglomerations of Upsalite particles were formed.

There was a clear difference in the mechanical properties between Klucel ELF and AquaSolve LG. The pure Klucel-filaments were more ductile upon bending, although showcasing a partially brittle fracture as the first half was deformed. However, in order to separate the two halves completely, either a torque or stretching force was necessarily applied. Due to its suitable mechanical properties for printing, no additives were used. Initially, two different mixtures consisting of the polymer combined with unloaded Upsalite and crystalline magnesium carbonate were extruded. The resulting filaments were more brittle as expected, but the moderate increase in stiffness combined with the inherent ductility of the polymer made it more suitable for printing compared to the AquaSolve-based filaments. Klucel ELF seemed to be more miscible with the Upsalite in regard to the material distribution, since the phenomena previously

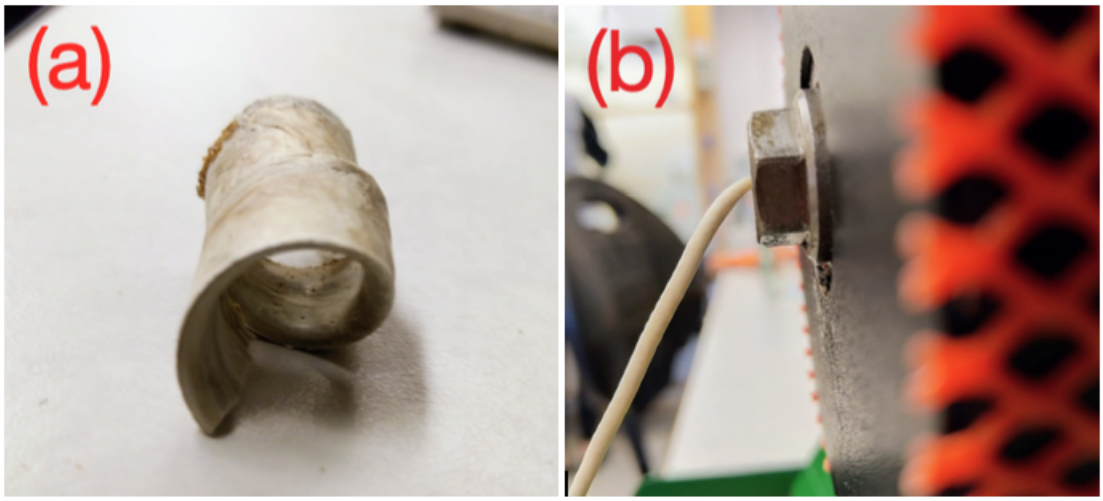

Figure 10: (a) Here, the coated layer inside the extruder is shown. It was mainly composed of the API-loaded Upsalite, due to its brittleness and the high degree of white powder that was observed when breaking the component apart into smaller fragments. (b) The prominent die-swell effect obtained during extrusion of the loaded AquaSolve-filament.

described were either observed to a non-significant degree or not at all. Interestingly, tablets based on the crystalline magnesium carbonate were successfully printed, opposed to the failed trials conducted with the unloaded Upsalite. Filaments of loaded Upsalite were extruded at 140°C and displayed an increase in toughness relative to the corresponding unloaded filament. The obtained filament had a smooth surface as can be seen in Figure 9 (b), and a good thickness control was achieved. Successful tablets with 30 wt% drug loaded Upsalite were continuously printed without any issues at 205°C and a bed temperature of 60°C, corresponding to a total drug loading of 2.60 wt%. This composition was used to print tablets with 100% and 50% infill densities (Figure 11), which were subsequently used for the dissolution studies. At later stages of the project, tablets containing 40 wt% API-loaded Upsalite were successfully printed as well.

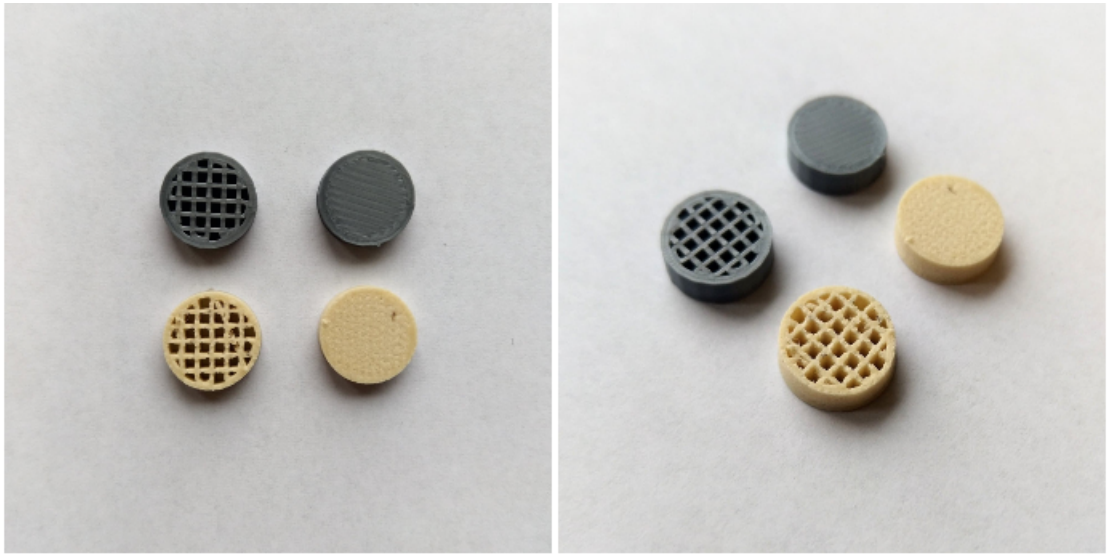

Figure 11: The comparison of printed tablets using a commercial PLA filament (grey) received from Prusa Research and the Klucel–based filament with 30 wt% API-loaded Upsalite.

4.3 Characterization of extrudates and tablets

In Figure 12, images taken with SEM of drug-loaded Upsalite particles, drug loaded Klucel filament and the successfully printed 50% infill tablet can be seen. The Upsalite particles were observed to have an irregular geometric shape (Figure 12 (a)) as previously seen, with sizes varying up to approximately 20 μm. Structural differences between the loaded– and unloaded Upsalite particles could not be distinguished. Figure (b) depicts the filament, which distinctively shows the Upsalite particles coated with an outer polymeric layer, thus creating a coarse surface on the microscale. The image of the 50% infill tablet taken from above shows the string–like morphology of solidified polymer melt, most probably as a result of the thin deposited layers being compressed and stretched by the movement of the printer head. Furthermore, the uncharacteristic layer that is seen extending diagonally through the grid holes were generated by the oozing of molten material through the nozzle as the printer head was moving, due to removal of the filament retraction function, which can also be macroscopically distinguished from the pictures on Figure 11. The last image, taken from the side of the 50% infill tablet, shows the distinctive layer–by–layer construction of the tablet.

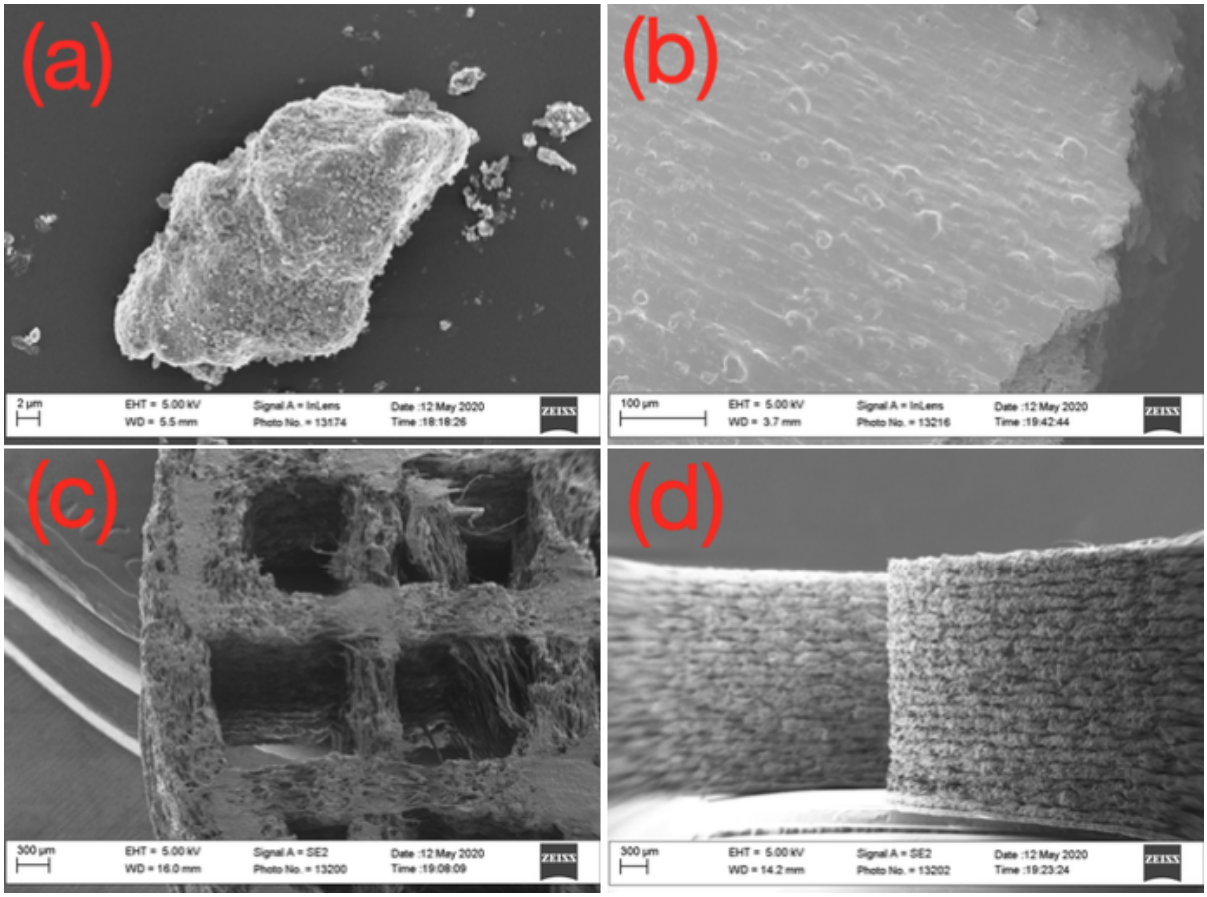

Figure 12: (a) The irregular geometry of unloaded Upsalite particles. (b) Depiction of the filament just at the edge of a cross section, showing the polymer coated Upsalite particles. (c) Image of the 50% infill tablet taken from above, showing the structure of the last polymer layer that was deposited. (d) Image of the same tablet but taken from the side, which shows the characteristic layer-by-layer structure of an FDM-printed object.

Figure 13 (a) shows the DSC-curves of cinnarizine, Klucel ELF, physical mixture, filament and the successfully printed tablet. Traces of the endothermic peak corresponding to the melting point of crystalline cinnarizine can still be observed at 121°C. Assuming that the drug was in fact partially crystallized during the loading procedure, the results indicate that the thermal treatments by extrusion and printing did not give rise to a possible interaction between the crystalline API and the polymer, as have been previously seen when hot-melt extrusion is utilized as a tool for creating amorphous solid dispersions. Furthermore, this is confirmed when observing the FTIR spectra, which remains unchanged for the filament and tablet as shown in Figure 13 (b).

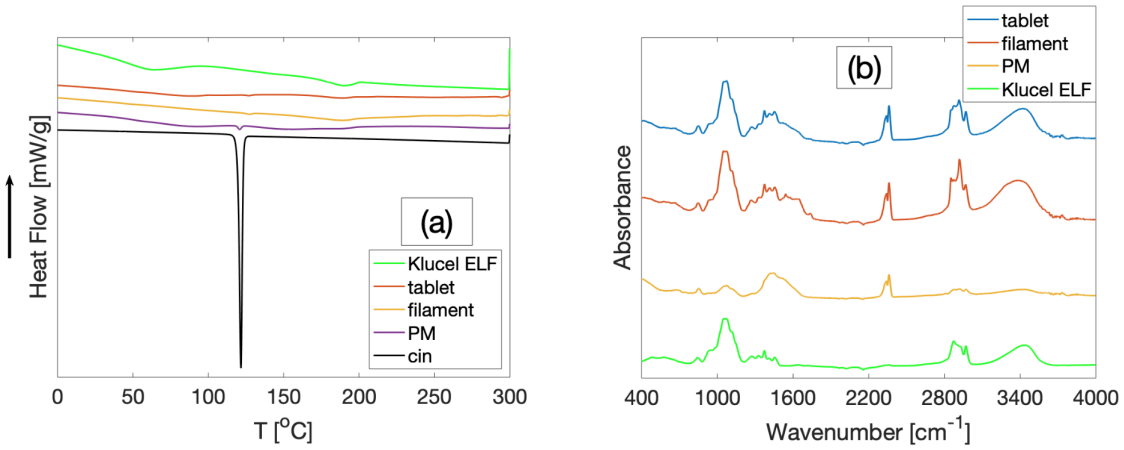

Figure 13: (a) The resulting DSC-curves from experiments conducted with the API, Klucel, physical mixture (denoted PM), filament and printed tablet. (b) Absorbance spectra for Klucel ELF, filament, tablet and the physical mixture (PM) of loaded Upsalite and Klucel.

TG-measurements on various components are shown in Figure 14. Decomposition of crystalline cinnarizine at 320°C suggests that no mass loss would occur at the temperatures used during extrusion and printing, although the API starts decomposing at a slow rate around 200°C. Commonly displayed for all samples are the small fractions of weight losses at 40°C, corresponding to evaporation of moisture. As can be observed in the TG-curves of loaded and unloaded Upsalite, the moisture content is higher in comparison to the other samples, which is due to its hygroscopic properties. In accordance with previous studies, magnesium carbonate was decomposed into MgO and CO_2 at a temperature around 363°C [26, 28, 29]. The mass loss due to the corresponding decomposition in API-loaded Upsalite was shifted towards 381°C, suggesting that the incorporation of drug into the pore network stabilizes the whole structure of Upsalite. This phenomenon lies is accordance with previous studies relating to the drug loading of Upsalite [26, 29, 30, 31].

The drug content in Upsalite can be determined by assigning weight losses attributed to the degradation of cinnarizine. In the TG-curve of loaded Upsalite, three different stages of weight loss can be discerned. Loss of moisture, loss of API and decomposition of Upsalite. The weight loss of the API occurs at temperatures between 195–332°C, corresponding to 7.71mwt%. Drug content in tablets can be obtained by calculating the difference between the final values of loaded and unloaded samples, generating a drug loading of 2.23 wt%. These values indicate a decrease in drug content with respect to the amounts used during the loading procedure, which is expected due to material loss arising from the aforementioned procedure, as well as the extrusion and the printing processes.

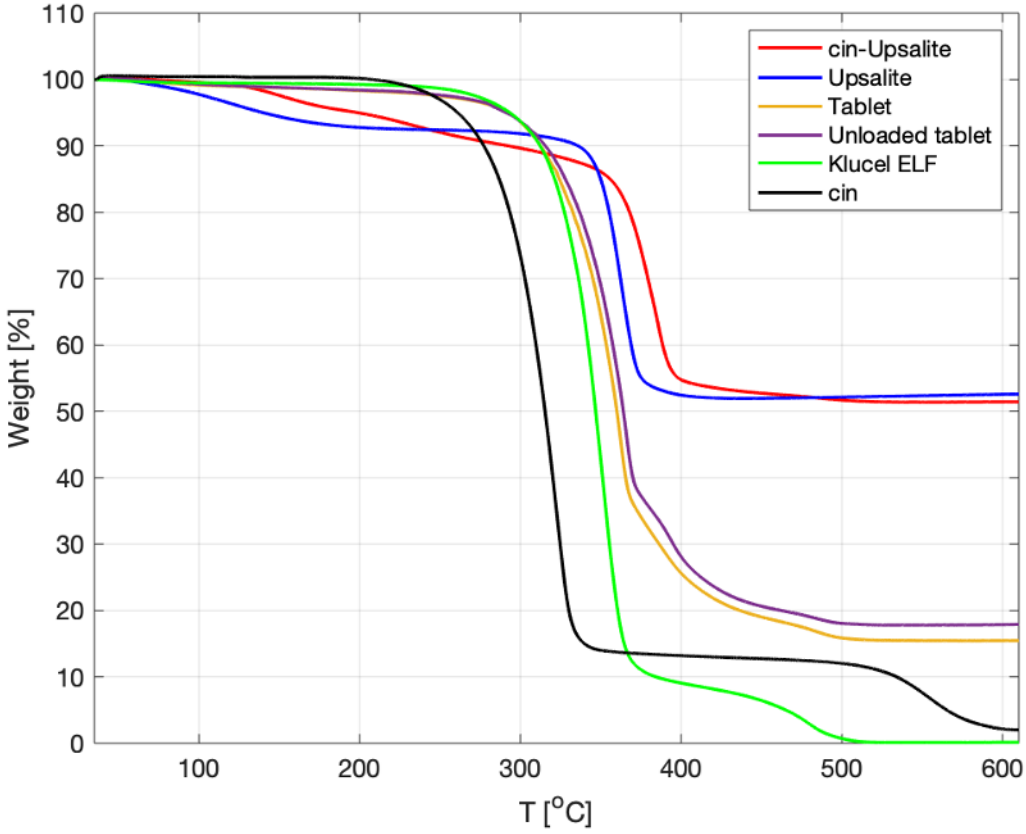

Figure 14: TG–curves with weight percentage as a function of temperature.

4.4 Drug release from printed tablets

Figure 15 shows the resulting dissolution curves of the crystalline API, loaded Upsalite and tablets. The two top figures correspond to dissolution tests on the tablet with 100% infill density and the two lower ones for the tablet with 50% infill density. The common trend for all experiments is that the dissolution rate of cinnarizine was the highest when incorporated into the Upsalite. The fast-dissolving character of the amorphous API is evident by its initial rapid release, which is in accordance with previously presented results. After 10 minutes, the average release rate of incorporate Upsalite was almost 2.5 times higher than the rate of crystalline API, which continued to be the case even after 30 minutes. The benefit of using Upsalite as a drug–release enhancing delivery vehicle is evident by the fact that the final concentration of crystalline drug after 8 hours (5 mg/L) was achieved in less than 50 minutes for the amorphous drug. One thing that has to be addressed is the occurrence of sharp concentration deviations for the crystalline–and amorphous drugs (corresponding to 100% infill loading) between the 2-hour–and 5-hour mark. The initial dip in concentration was obtained when the previously used filter was replaced with a new one mid-testing, thus, the filter remained unchanged for the remaining measurements in order to avoid this discrepancy. Worth noting is that the concentration values in-between the 2-hour–and 5-hour mark can be approximated by linear interpolation, as indicated by the release profiles of corresponding compounds in the 50% infill study. The dissolution of incorporated API did not result in a supersaturated state due to the experiments being conducted under sink conditions, meaning that the volume of the dissolution media should be able to dissolve 3 times the amount of drug that is contained within the delivery system. The

measured concentration from the solubility study was around 25 mg/L, which is more than 3 times higher than the maximum amount dissolved in these studies (7 mg/L).

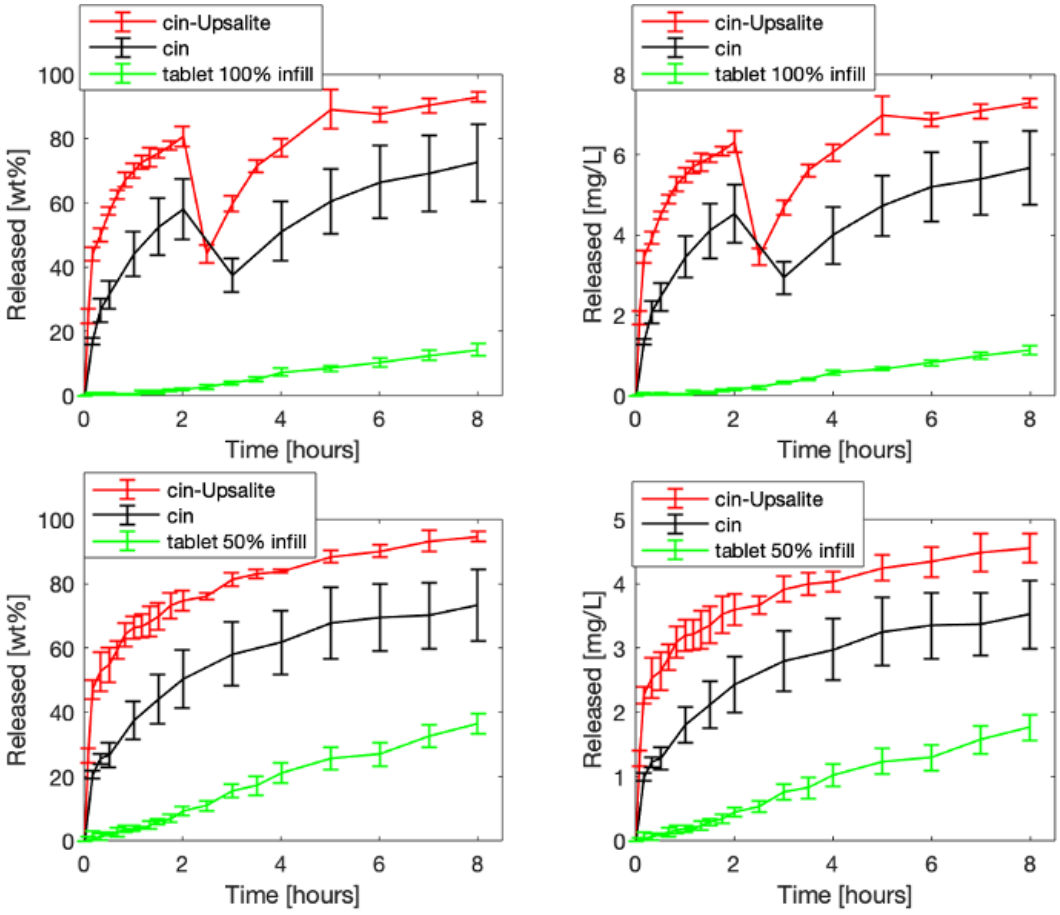

Figure 15: Upper graphs: Dissolution curves for the 100% infill tablet, API-loaded Upsalite and crystalline cinnarizine are expressed as the mass percentage released and the concentration released as a function of time. Bottom graphs: Experiments conducted on the same compounds, with the only difference being that they correspond to 50% infill density.

Dissolution of API from the tablets had a slower rate than the crystalline API throughout the whole experiment. One parameter that has to be accounted for is that the API was contained within a densified polymer matrix that constitutes the tablet. As a result, the total surface area of the solute interacting with the solvent is reduced in comparison to the powdered crystalline API-samples. However, the release of API from the printed tablets seems to be largely dependent on the dissolution of the polymeric matrix. The slow drug release from the tablet can most probably be attributed to the slower dissolution rate of the polymer in relation to the amorphous drug itself. More specifically, since the dissolution mechanism of the polymer is firstly based on swelling, the polymer needs to absorb solvent molecules in order for the solvent–API interaction to occur. Furthermore, in cases when the polymer is not readily dissolved through the erosion process, the release of dissolved drug molecules from the polymer matrix is controlled by their diffusion through polymeric layers [56].

The purpose of printing tablets with different infill densities was to study the change in dissolution characteristics when increasing the total surface area of the tablet. As expected, the 50% infill tablet displayed an increase in dissolution rate. After 8 hours, approximately 14.3% of API was released from the 100% infill tablet, whereas the same fraction was released in under three hours from the 50% infill tablet. This was also visually observed during the experiment, in which the degree of swelling was more prominent in the 50% infill tablet. Images on the swelled tablets where taken at different stages of the experiment and are presented in figure 16. Both dissolution curves display a more or less linear release behavior, which eventually changed sometime in between the 8– and 24 hours into the study, resulting in a profile characteristic of the ones obtained during dissolution of the crystalline drug and loaded Upsalite, i.e. with a release rate decreasing over time.

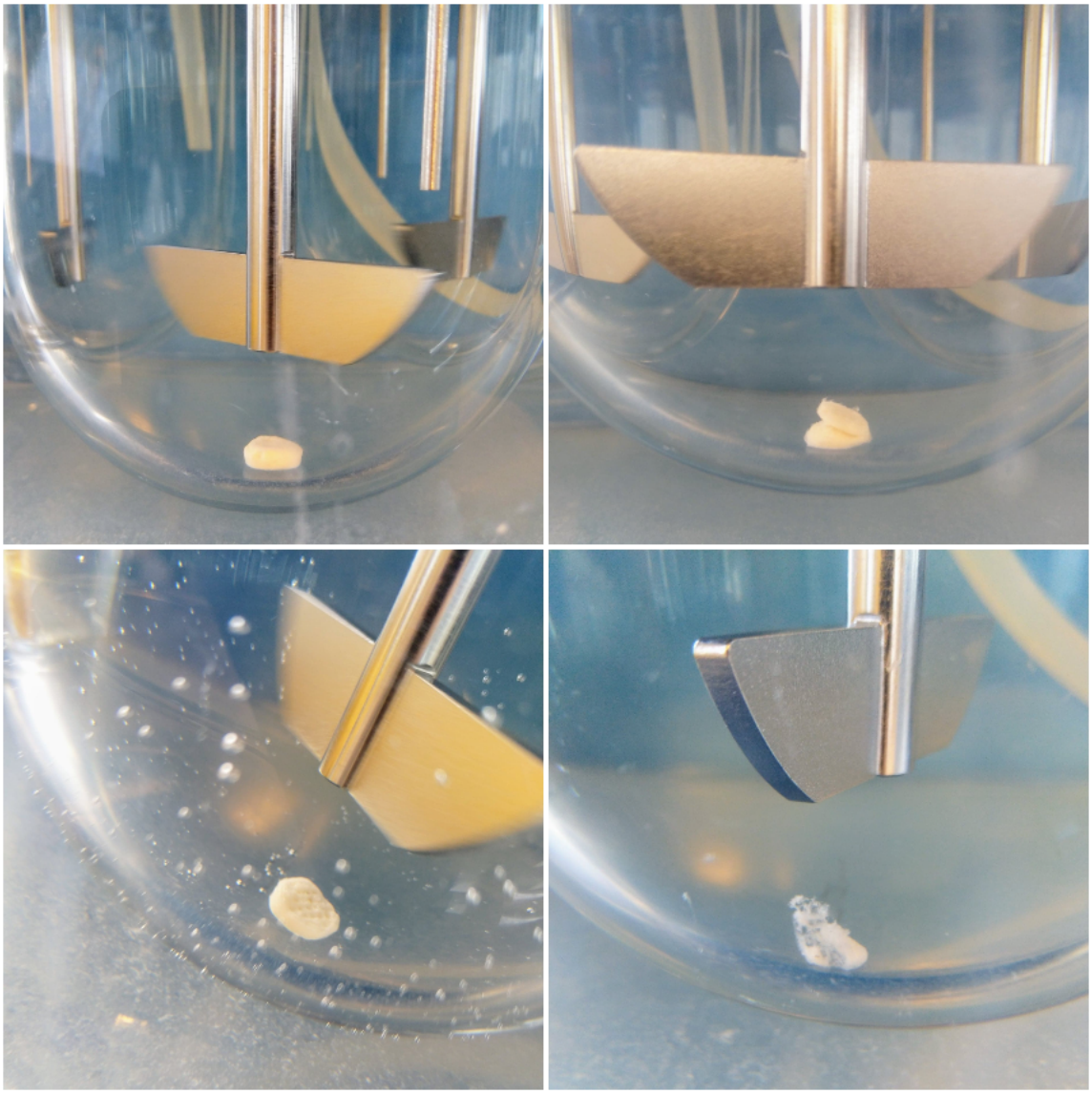

Figure 16: Upper images show one of the 100% infill tablets after 3 hours (left) and 24 hours (right). The images below correspond to a 50% infill tablet after 1 hour (left) and 24 hours (right).

5 Conclusion

Cinnarizine was incorporated into the pores of mesoporous magnesium carbonate (Upsalite) via a soaking method, corresponding to a drug loading of 8.67 wt%. XRD-measurements showed that crystallization of the drug was suppressed, in contrast to DSC-measurements, indicating the presence of a crystalline phase. The drug-loaded material was hot-melt extruded with the pharmaceutical polymers AquaSolve LG and Klucel ELF. AquaSolve filaments were brittle and showcased a non-uniform dispersion of Upsalite particles within the polymer melt, opposed to the Klucel filament, which was macroscopically homogenous. Printing trials were conducted on each filament, with the AquaSolve filament failing to produce tablets due to clogging of the printer head, which is most likely explained by the non-optimal properties (e.g. thickness variations, uneven material distribution, brittleness). Drug-loaded Klucel filaments (2.60 wt% cinnarizine) were successfully utilized for printing tablets. TGA conducted on loaded materials suggests a drug loading of 7.71 wt% and 2.23 wt% in Upsalite and tablet respectively. Release studies of respective infill tablet, crystalline API and drug-loaded Upsalite were conducted in an USP II apparatus containing a PBS-based buffer solution. The study entailed a slower dissolution of drug species from the tablets compared to corresponding crystalline API samples, most probably due to differences in total surface area and slow dissolution of Klucel ELF.

6 Future perspective

Even though drug loaded Upsalite was coupled with a pharmaceutical polymer in Klucel ELF to successfully print tablets, there can still be further improvements. With regards to printing, the process is mainly dependent on the filament properties. In this study, single screw extrusion of AquaSolve and drug-loaded Upsalite resulted in non-suitable filaments mainly due to non-optimal material distributions. This issue can most probably be resolved to a certain extent by imposing shear deformation onto the molten mixture by utilizing a twin-screw extruder, which would enable a more homogenous dispersion of Upsalite particles within the polymer melt. The choice of polymer can also be addressed with respect to its dissolution properties and the desired release profile. Pharmaceutical grade polymers that exhibit higher aqueous solubility (e.g. Plasdone S-630, PVP K12, Soluplus) should be investigated more in depth in order to minimize the inhibiting effect on the immediate release property of the mesoporous drug carrier. Furthermore, the issue could also be approached from the perspective of designing dosage forms that exploit the properties of Upsalite more efficiently, e.g. printing thin-walled hollow polymeric tablets filled with drug-loaded Upsalite powder.

References

[1] Thomas N Tozer and Malcolm Rowland. *Essentials of pharmacokinetics and pharmacodynamics*. 2016, pp. 23–24, 52.

[2] Joachim Brouwers, Marcus E Brewster, and Patrick Augustijns. "Supersaturating drug delivery systems: the answer to solubility-limited oral bioavailability?" In: *Journal of pharmaceutical sciences* 98.8 (2009), pp. 2549–2572.

[3] Alice Melocchi et al. "Hot-melt extruded filaments based on pharmaceutical grade polymers for 3D printing by fused deposition modeling". In: *International journal of pharmaceutics* 509.1-2 (2016), pp. 255–263.

[4] Michael E Aulton. "Pharmaceutics: the science of dosage form design. 2002". In: (), pp. 16–19.

[5] Arthur A Noyes and Willis R Whitney. "The rate of solution of solid substances in their own solutions." In: *Journal of the American Chemical Society* 19.12 (1897), pp. 930–934.

[6] Gordon L Amidon et al. "A theoretical basis for a biopharmaceutic drug classification: the correlation of in vitro drug product dissolution and in vivo bioavailability". In: *Pharmaceutical research* 12.3 (1995), pp. 413–420.

[7] Peter Atkins and Loretta Jones. *Chemical principles: The quest for insight*. Macmillan, 2007, pp. 298–300, 384–387.

[8] Michael E Aulton and Kevin MG Taylor. *Aulton's Pharmaceutics E-Book: The Design and Manufacture of Medicines*. Elsevier Health Sciences, 2017, p. 403.

[9] Khadijah Edueng et al. "Supersaturation potential of amorphous active pharmaceutical ingredients after long-term storage". In: *Molecules* 24.15 (2019), p. 2731.

[10] Kerstin Frank et al. "Amorphous solid dispersion enhances permeation of poorly soluble ABT-102: True supersaturation vs. apparent solubility enhancement". In: *International journal of pharmaceutics* 437 (Aug. 2012), pp. 288–93. DOI: 10.1016/j.ijpharm.2012.08.014.

[11] Arik Dahan et al. "The twofold advantage of the amorphous form as an oral drug delivery practice for lipophilic compounds: increased apparent solubility and drug flux through the intestinal membrane". In: *The AAPS journal* 15.2 (2013), pp. 347–353.

[12] Kerstin J Frank et al. "What is the mechanism behind increased permeation rate of a poorly soluble drug from aqueous dispersions of an amorphous solid dispersion?" In: *Journal of Pharmaceutical Sciences* 103.6 (2014), pp. 1779–1786.

[13] YOSHINOBU NAKAI et al. "Interaction of medicinals and porous powder. I. Anomalous thermal behavior of porous glass mixtures". In: *Chemical and pharmaceutical bulletin* 32.11 (1984), pp. 4566–4571.

[14] Yoshinobu NAKAI, Keiji YAMAMOTO, and Satoshi IZUMIKAWA. "Interaction of Medicinals and Porous Powder. III.: Effects of Pore Diameter of Porous Glass Powder on Crystalline Properties". In: *Chemical and pharmaceutical bulletin* 37.2 (1989), pp. 435–438.

[15] M Vallet-Regi et al. "A new property of MCM-41: drug delivery system". In: *Chemistry of Materials* 13.2 (2001), pp. 308–311.

[16] Shou-Cang Shen et al. “Stabilized amorphous state of ibuprofen by co-spray drying with mesoporous SBA-15 to enhance dissolution properties”. In: *Journal of pharmaceutical sciences* 99.4 (2010), pp. 1997–2007.

[17] Ana R Brás et al. “Amorphous ibuprofen confined in nanostructured silica materials: a dynamical approach”. In: *The Journal of Physical Chemistry C* 115.11 (2011), pp. 4616–4623.

[18] Agnes Szegedi et al. “Controlled drug release on amine functionalized spherical MCM-41”. In: *Journal of Solid State Chemistry* 194 (2012), pp. 257–263.

[19] Corine Gérardin et al. “Ecodesign of ordered mesoporous silica materials”. In: *Chemical Society Reviews* 42.9 (2013), pp. 4217–4255.

[20] Ken K Qian and Robin H Bogner. “Spontaneous crystalline-to-amorphous phase transformation of organic or medicinal compounds in the presence of porous media, part 1: thermodynamics of spontaneous amorphization”. In: *Journal of pharmaceutical sciences* 100.7 (2011), pp. 2801–2815.

[21] Ken K Qian and Robin H Bogner. “Application of mesoporous silicon dioxide and silicate in oral amorphous drug delivery systems”. In: *Journal of pharmaceutical sciences* 101.2 (2012), pp. 444–463.

[22] Nele-Johanna Hempel et al. “A fast and reliable DSC-based method to determine the monomolecular loading capacity of drugs with good glass-forming ability in mesoporous silica”. In: *International Journal of Pharmaceutics* 544.1 (2018), pp. 153–157.

[23] GT Rengarajan et al. “Stabilization of the amorphous state of pharmaceuticals in nanopores”. In: *Journal of Materials Chemistry* 18.22 (2008), pp. 2537–2539.

[24] Christoffer G Bavnhøj et al. “The role interplay between mesoporous silica pore volume and surface area and their effect on drug loading capacity”. In: *International Journal of Pharmaceutics: X* 1 (2019), p. 100008.

[25] Yin Yani, Pui Shan Chow, and Reginald BH Tan. “Pore size effect on the stabilization of amorphous drug in a mesoporous material: insights from molecular simulation”. In: *Microporous and Mesoporous Materials* 221 (2016), pp. 117–122.

[26] Peng Zhang et al. “Diffusion-controlled drug release from the mesoporous magnesium carbonate Upsalite®”. In: *Journal of Pharmaceutical Sciences* 105.2 (2016), pp. 657–663.

[27] Johan Forsgren et al. “A template-free, ultra-adsorbing, high surface area carbonate nanostructure”. In: *PLoS One* 8.7 (2013), e68486.

[28] Sara Frykstrand et al. “On the pore forming mechanism of Upsalite, a micro-and mesoporous magnesium carbonate”. In: *Microporous and mesoporous materials* 190 (2014), pp. 99–104.

[29] Peng Zhang, Johan Forsgren, and Maria Strømme. “Stabilisation of amorphous ibuprofen in Upsalite, a mesoporous magnesium carbonate, as an approach to increasing the aqueous solubility of poorly soluble drugs”. In: *International journal of pharmaceutics* 472.1-2 (2014), pp. 185–191.

[30] Peng Zhang et al. “Supersaturation of poorly soluble drugs induced by mesoporous magnesium carbonate”. In: *European Journal of Pharmaceutical Sciences* 93 (2016), pp. 468–474.

[31] Jiaojiao Yang et al. “Enhanced release of poorly water-soluble drugs from synergy between mesoporous magnesium carbonate and polymers”. In: *International Journal of Pharmaceutics* 525.1 (2017), pp. 183–190.

[32] Deck Khong Tan, Mohammed Maniruzzaman, and Ali Nokhodchi. “Advanced pharmaceutical applications of hot-melt extrusion coupled with fused deposition modelling (FDM) 3D printing for personalised drug delivery”. In: *Pharmaceutics* 10.4 (2018), p. 203.

[33] Alvaro Goyanes et al. “Fabrication of controlled-release budesonide tablets via desktop (FDM) 3D printing”. In: *International journal of pharmaceutics* 496.2 (2015), pp. 414–420.

[34] Alvaro Goyanes et al. “Fused-filament 3D printing (3DP) for fabrication of tablets”. In: *International journal of pharmaceutics* 476.1-2 (2014), pp. 88–92.

[35] Justyna Skowyra, Katarzyna Pietrzak, and Mohamed A Alhnan. “Fabrication of extended-release patient-tailored prednisolone tablets via fused deposition modelling (FDM) 3D printing”. In: *European Journal of Pharmaceutical Sciences* 68 (2015), pp. 11–17.

[36] Alvaro Goyanes et al. “3D printing of modified-release aminosalicylate (4-ASA and 5-ASA) tablets”. In: *European Journal of Pharmaceutics and Biopharmaceutics* 89 (2015), pp. 157–162.

[37] Alvaro Goyanes et al. “Effect of geometry on drug release from 3D printed tablets”. In: *International journal of pharmaceutics* 494.2 (2015), pp. 657–663.

[38] Alvaro Goyanes et al. “Direct powder extrusion 3D printing: Fabrication of drug products using a novel single-step process”. In: *International journal of pharmaceutics* 567 (2019), p. 118471.

[39] Katarzyna Pietrzak, Abdullah Isreb, and Mohamed A Alhnan. “A flexible-dose dispenser for immediate and extended release 3D printed tablets”. In: *European journal of pharmaceutics and biopharmaceutics* 96 (2015), pp. 380–387.

[40] Alvaro Goyanes et al. “Development of modified release 3D printed tablets (printlets) with pharmaceutical excipients using additive manufacturing”. In: *International journal of pharmaceutics* 527.1-2 (2017), pp. 21–30.

[41] Andrew J Peacock and Allison Calhoun. *Polymer Chemistry: Properties and Application*. Carl Hanser Verlag GmbH Co KG, 2012, pp. 23–24, 52.

[42] Milind Vasant Kirtane et al. “Cinnarizine: a contemporary review”. In: *Indian Journal of Otolaryngology and Head & Neck Surgery* 71.2 (2019), pp. 1060–1068.

[43] Mark Berlin et al. “Prediction of oral absorption of cinnarizine–a highly supersaturating poorly soluble weak base with borderline permeability”. In: *European Journal of Pharmaceutics and Biopharmaceutics* 88.3 (2014), pp. 795–806.

[44] Chong-Hui Gu et al. “Using a novel multicompartment dissolution system to predict the effect of gastric pH on the oral absorption of weak bases with poor intrinsic solubility”. In: *Journal of pharmaceutical sciences* 94.1 (2005), pp. 199–208.

[45] Jonas H Fagerberg, Erik Sjögren, and Christel AS Bergström. “Concomitant intake of alcohol may increase the absorption of poorly soluble drugs”. In: *European Journal of Pharmaceutical Sciences* 67 (2015), pp. 12–20.

[46] *Ashland | Klucel^{TM} hydroxypropylcellulose*. Accessed 2020-07-07. URL: https://www.ashland.com/industries/pharmaceutical/oral-solid-dose/klucel-hydroxypropylcellulose.

[47] Alice Melocchi et al. "3D printing by fused deposition modeling (FDM) of a swellable/erodible capsular device for oral pulsatile release of drugs". In: *Journal of Drug Delivery Science and Technology* 30 (2015), pp. 360–367.

[48] Jiaxiang Zhang et al. "Coupling 3D printing with hot-melt extrusion to produce controlled-release tablets". In: *International journal of pharmaceutics* 519.1-2 (2017), pp. 186–197.

[49] Basel Arafat et al. "Tablet fragmentation without a disintegrant: A novel design approach for accelerating disintegration and drug release from 3D printed cellulosic tablets". In: *European Journal of Pharmaceutical Sciences* 118 (2018), pp. 191–199.

[50] Shiva Homaee Borujeni et al. "Three-dimensional (3D) printed tablets using ethyl cellulose and hydroxypropyl cellulose to achieve zero order sustained release profile". In: *Cellulose* 27.3 (2020), pp. 1573–1589.

[51] *Ashland | AquaSolve^{TM} hypromellose acetate succinate.* Accessed 2020-07-07. URL: https://www.ashland.com/industries/pharmaceutical/oral-solid-dose/aquasolve-hypromellose-acetate-succinate..

[52] Dwayne T Friesen et al. "Hydroxypropyl methylcellulose acetate succinate-based spray-dried dispersions: an overview". In: *Molecular pharmaceutics* 5.6 (2008), pp. 1003–1019.

[53] William Curatolo, James A Nightingale, and Scott M Herbig. "Utility of hydroxypropylmethylcellulose acetate succinate (HPMCAS) for initiation and maintenance of drug supersaturation in the GI milieu". In: *Pharmaceutical research* 26.6 (2009), pp. 1419–1431.

[54] Jared A Baird, Bernard Van Eerdenbrugh, and Lynne S Taylor. "A classification system to assess the crystallization tendency of organic molecules from undercooled melts". In: *Journal of pharmaceutical sciences* 99.9 (2010), pp. 3787–3806.

[55] Johanna Aho et al. "Rheology as a tool for evaluation of melt processability of innovative dosage forms". In: *International journal of pharmaceutics* 494.2 (2015), pp. 623–642.

[56] Richard W Korsmeyer, Steven R Lustig, and Nikolaos A Peppas. "Solute and penetrant diffusion in swellable polymers. I. Mathematical modeling". In: *Journal of Polymer Science Part B: Polymer Physics* 24.2 (1986), pp. 395–408.

Appendix

Table 4: The various compositions (denoted C) studied with extrusion, given in weight percentage.

	AquaSolve LG	Klucel ELF	Magnesium carbonate	Unloaded Upsalite	Loaded Upsalite	PEG 400	Magnesium stearate
C1	100	–	–	–	–	–	–
C2	95	–	–	–	–	5	–
C3	90	–	–	–	–	10	–
C4	85	–	–	–	–	15	–
C5	65	–	20	–	–	15	–
C6	55	–	30	–	–	15	–
C7	55	–	–	30	–	15	–
C8	50	–	–	30	–	15	5
C9	55	–	–	–	30	15	–
C10	50	–	–	–	30	15	5
C11	–	100	–	–	–	–	–
C12	–	80	20	–	–	–	–
C13	–	70	30	–	–	–	–
C14	–	80	–	20	–	–	–
C15	–	70	–	30	–	–	–
C16	–	80	–	–	20	–	–
C17	–	70	–	–	30	–	–
C18	–	60	–	–	40	–	–

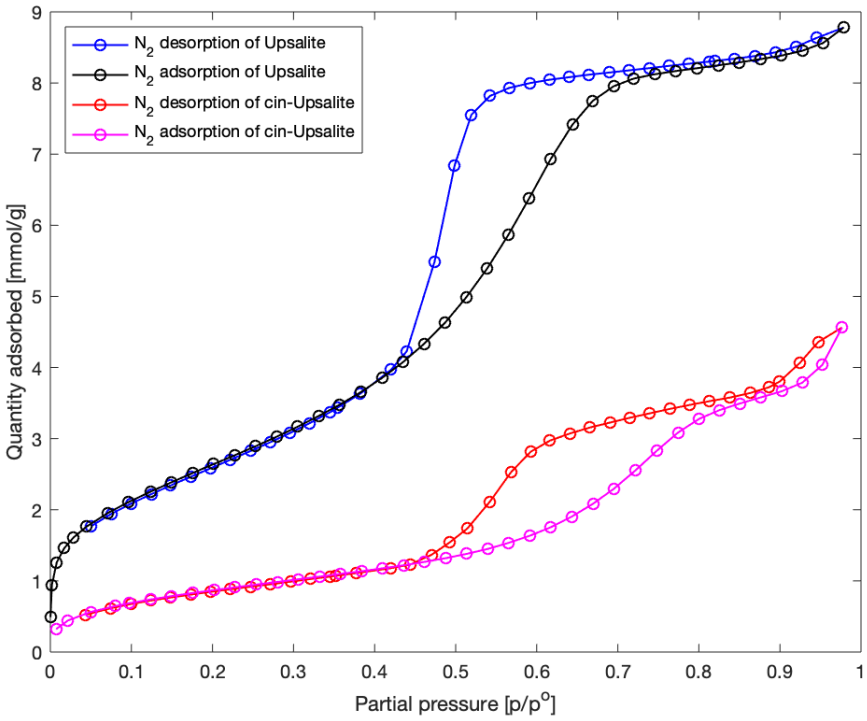

Figure 17: Isotherms for the API–loaded– and unloaded Upsalite.

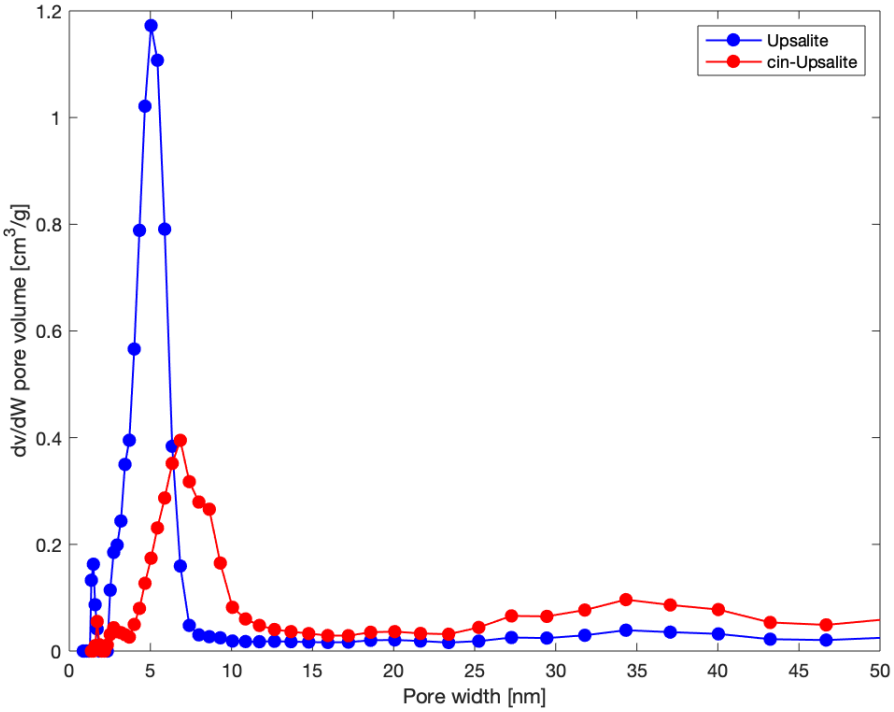

Figure 18: Pore–size distribution obtained by the N_2 sorption measurement.

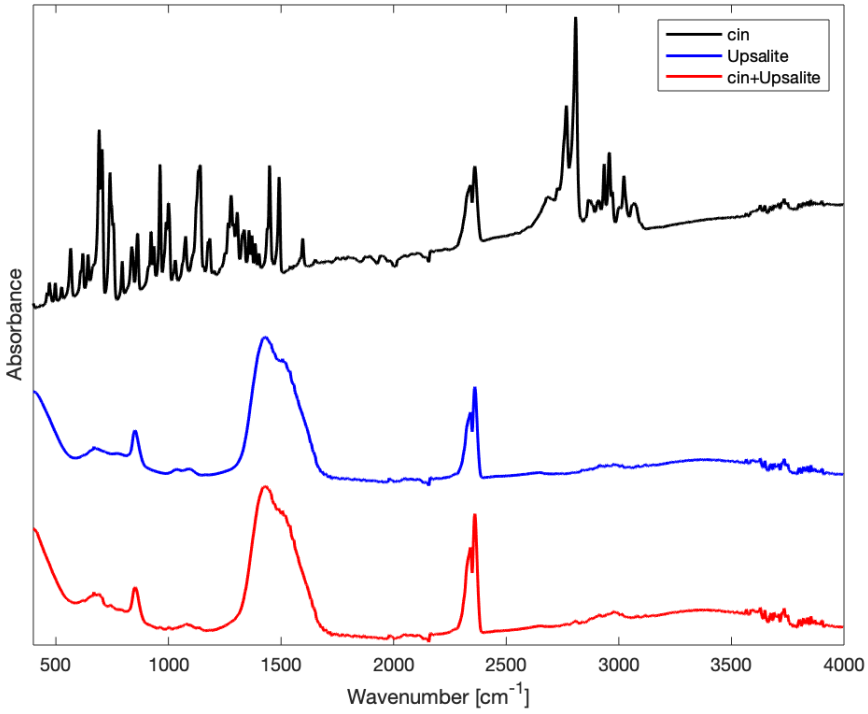

Figure 19: FTIR spectrum for cinnarizine, unloaded– and loaded Upsalite.

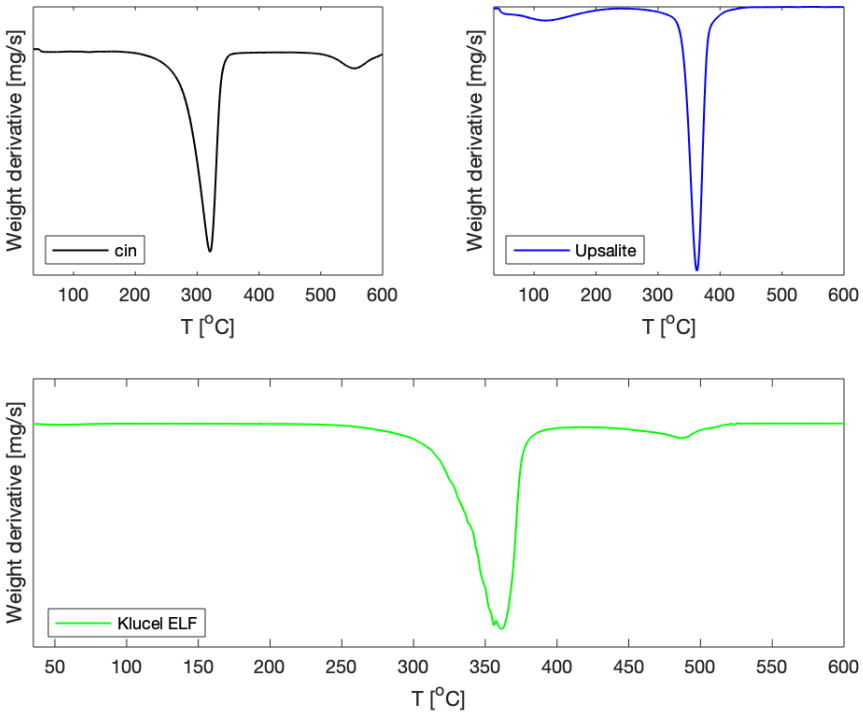

Figure 20: First derivative TG measurements on raw materials.

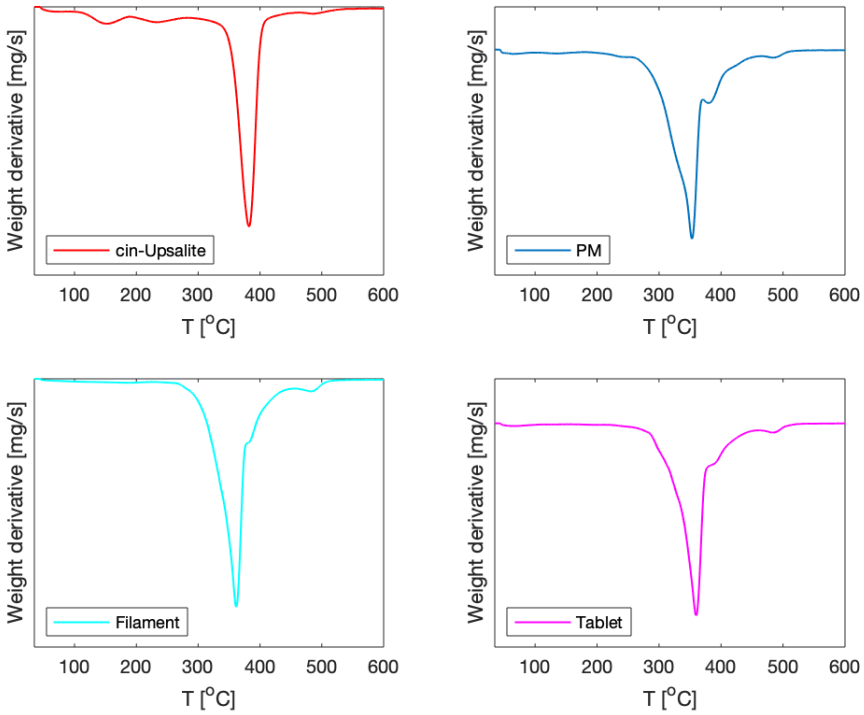

Figure 21: First derivative TG measurements on API-loaded components

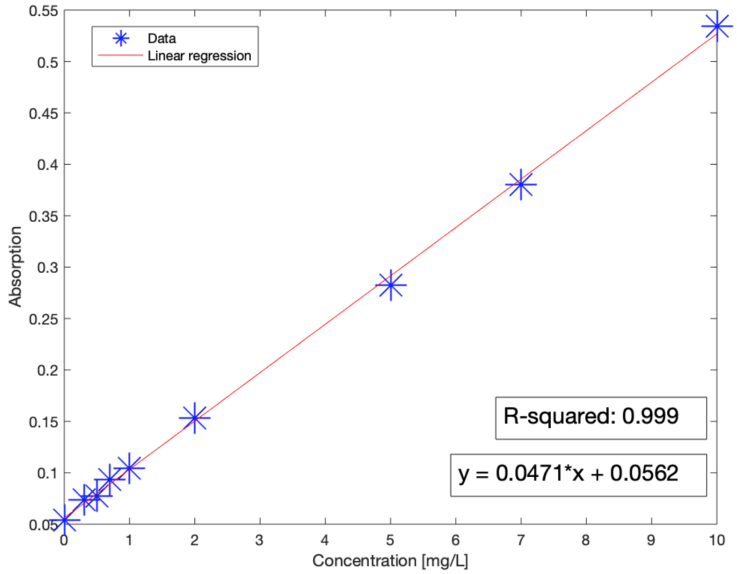

Figure 22: Calibration curve recorded for cinnarizine dissolved in 0.1M PBS and 0.05wt% SLS.